CHARACTERIZATION OF NEW NATURAL CELLULOSIC FIBRE FROM *LASIA SPINOSA* (L.) THWAITES RHIZOME FOR BIODEGRADABLE TEXTILE MATERIAL

M.H.Methmini Tharanga Rathnapala

168306M

Degree of Master of Science in Textile and Clothing Management

Department of Textile and Clothing Technology

University of Moratuwa

Sri Lanka

July 2020

CHARACTERIZATION OF NEW NATURAL CELLULOSIC FIBRE FROM *LASIA SPINOSA* (L.) THWAITES RHIZOME FOR BIODEGRADABLE TEXTILE MATERIAL

M.H.Methmini Tharanga Rathnapala

168306M

Dissertation submitted in partial fulfillment of the requirements for the degree of Master of Science in Textile and Clothing Management

Department of Textile and Clothing Technology

University of Moratuwa

Sri Lanka

July 2020

Declaration

I declare that this is my own work and this dissertation does not incorporate without acknowledgement any material previously submitted for a Degree or Diploma in any other University or institute of higher learning and to the best of my knowledge and belief it does not contain any material previously published or written by another person except where the acknowledgement is made in the text.

Also, I hereby grant to University of Moratuwa the non-exclusive right to reproduce and distribute my dissertation, in whole or in part in print, electronic or other medium. I retain the right to use this content in whole or part in future works (such as articles or books).

Signature: Date:

The above candidate has carried out research for the Masters Dissertation under my supervision.

Name of the supervisor:

Signature of the supervisor: Date :

Acknowledgement

From the beginning to the end of this research journey I was supported by number of incredible people with their fullest support to bringing this research to a successful level. I would like to express my sincere gratitude to all who have guided and supported me to make this research a success.

Foremost, I express the deepest appreciation to my supervisor, Dr. U.S.W.Gunasekera for his continuous encouragement, guidance, patience, knowledge and for being a great adviser throughout the research period.

I am grateful to the former and present research coordinators, Dr.T.S.S.Jayawardene and Dr.Ranga Abeysooriya of the Department of Textile and Clothing Technology for adding the platform for the conduct of this research and supporting until the final submission and thankful to all the lecturers of the MSc program for sharing their expertise, valuable encouragement and support extended to me in completing the course.

I would deeply grateful to Dr.Shantha Amarasinghe of the Department of Materials Science and Engineering for allowing me to conduct testing of the research with the equipment belongs to the respective department.

I would like to thank Technical Officers, Mr.C.P.Malalanayake and Mrs. D.S. Dissanayake of the Department of Textile and Mr. M.A.P.C.Gunawardana and Mr. M.T.M.R. Jayaweera of the Department of Material Science for their support rendered in laboratory testing with greater helping hand.

I would also like to thank Ms.Nadeeka Thissera, Senior Research Assistant of SLINTEC for her kind support in providing guidance for data analysis taking time from her busy schedules. Further express my gratitude to Mr. G.H.D.Wijesena, Post Graduate Course Administrator for his patience and support given to me throughout the whole study period with a kind helping hand.

Last but not least, I am deeply grateful to my mother and my husband for their continuous support in completing my research.

Abstract

This study presents the characteristics of *Lasia spinosa* fibres (LSFs) extracted from the rhizome of the *Lasia spinosa* (L.) Thwaites (LS), a plant which is commonly available in the Asian region as a medicinal plant which has not been investigated previously with the intension of exploring the feasibility in developing a textile material. Two common species, Lamina dissected type and Sagittate type plant rhizome fibres were investigated with the use of fibre characterization tools and methods. Mechanical extraction and Alkali extraction methods were followed in extracting fibres from rhizomes. Morphological properties of fibres such as longitudinal section and cross section views were studied using Scanning Electron Microscopy (SEM). Chemical functional groups and crystalline structure, were investigated using Fourier Transform Infrared Spectroscopy (FTIR) and X-Ray Diffraction analysis (XRD) respectively. Thermal stability of the fibre was investigated using Thermogravimetric Analyzer (TGA). In addition, fibre properties were investigated by the way of measuring tensile properties, moisture absorbency and dye uptake.

The rhizome anatomy and the fibre morphological observations through SEM reveals fibres are presents in rhizome in the form of scattered vascular bundles with crimp. Each bundle contains approximately 16-25 microfibrils. The FTIR analysis confirms the fibres are rich in cellulose and the X-RD results confirm higher amount of amorphous regions in fibres with a crystallinity index of 43% with a lower amount of crystal phases. Higher moisture regains of 12.54 -14.5%, single fibre tensile strength of 201-205 MPa, higher breaking elongation of 16.89% and 1.3 GPa of Young's modulus with a thermal stability temperature of 230℃ were the some of the values obtained in this research project. All the results obtained were compared with the characteristics of Cotton fibre.

Table of contents

List of figures

Page

List of tables

Page

List of abbreviations

Abbreviation	Description
LS	*Lasia spinosa*
LD	Lamina Dissected
SG	Sagittate
LDTF	Lamina Dissected Type Fibre
SGF	Sagittate Type Fibre
EAF	*Epipremnum aureum* fibres
SEM	Scanning Electron Microscopy
TEM	Transmission Electron Microscopy
FTIR	Fourier Transform Infrared Spectroscopy
XRD	X-Ray Diffractometer
CI	Crystallinity Index
CS	Crystal size

List of appendices

CHAPTER 1: INTRODUCTION

1.1 Background of the study

Numerous authors and researchers have emphasized the environmental issues that are occurred due to the use of chemicals and non-renewable natural resources such as fossil fuels in the synthetic textile manufacturing processors. According to Blackburn [1], the world population is predicted to increase up to ten billion by 2050 and an increased need for textiles. Hence, it is expected a comparable boost of synthetic textile manufacturing and an increase of the emissions of pollutants in to the environment and a decrease of limited resources such as fossil fuels.

A huge environmental pollution occurs such as translocation of carbon to the atmosphere, release of Sulphur and nitrogen oxides as well as all kinds of hydrocarbons and heavy metals due to the use of fossil fuels during the energy generation in manufacturing synthetic textile fibres. Further the fossil fuels are considered as a source of anthropogenic greenhouse gases that are widely contributed to the global warming which leads to frequent and extreme climate changes such as floods, droughts, heat waves, wind-storms, ice-storms, hurricanes and cyclones. Many of the harmful environmental challenges have occurred, such as sea level rising, air and water pollution, the spread of diseases that cause deaths for humans like malaria, yellow fever, migration of species and wildfires [1].

Textiles made out of synthetic fibres are durable in use. However, they are not degraded readily once they are released to the environment. As a result of that, land fill is increasing and reduces the spaces that are available for the dispose of waste [1].

According to the research done by Fletcher [2], on sustainability challenges of manufacturing textile materials, both plant and animal fibres are measured as environmentally friendly and synthetically manufactured fibres as non-friendly due to the non-renewability of the raw materials that are used, lower biodegradability and effect of pollutions to the environment as of the use of chemicals and processes applied in manufacturing of them.

These environmental impacts have become social and ethical concerns of some developed countries. According to Fletcher [2], carbon emissions has become a consideration of the UK and that has led to a rise in using carbon-neutral fibres such as bamboo, viscose and lyocell. In addition to the use of carbon-neutral fibres, the use of biodegradable fibres that are manufactured by the use of renewable resources has become popular as they are biodegradable and environmentally friendly. This attempt influences to move on with a variety of cellulosic fibres such as cotton and lyocell, and biodegradable synthetics made from plants, such as soy bean fibre and PLA from corn starch instead oil based synthetic fibres [2].

According to Muthu [3], there is a movement in manufacturing textile products with the use of natural fibres, maintaining sustainable processes from the production to the disposal of the materials. Essential properties such as good moisture absorbency, breathability, good strength, low weight, skin friendly and good thermal stability that are in natural fibres are driving the researchers to investigate novel natural fibres. As a result, researchers focused their attention on to investigate agricultural waste materials to extract fibres. Renewability, biodegradability, recyclability, and economical properties that exist on those fibres are the prime reasons for selecting them.

In recent studies, many of the researchers have investigated new natural cellulosic fibres by characterizing them to look for the possibilities of using them for the manufacturing of textiles and as reinforcing materials in composites.

1.2 Research problem

Sri Lanka is a tropical country which is having good climate condition throughout the whole year with many of the native plants that are unique to the South Asian region. Most of the natural plants that are globally used in textile manufacturing, such as cotton, lotus, bamboo, banana, jute and pineapple are fast growing plants in the soil conditions of Sri Lanka and many of the textile researchers in Sri Lanka have explored the characteristics of those fibres to investigate the possibility of manufacturing textiles from those plant fibres. Researchers are encouraged to investigate new plant fibres by the rising global

demand for cellulose fibre base textiles that are environmentally friendly, biodegradable and renewable. End uses of biodegradable textiles are varied such as manufacture of day today wearable apparels, geo-textiles and also medicinal textiles. In Sri Lanka there are fibre rich plants that are not yet been investigated with the intension of manufacturing textile materials. Initially the characteristics of the newly found plant fibres are to be investigated to decide the possibility of manufacturing textiles. End use of the plant fibres to be decided by the characterization of the respective fibres.

1.3 Focus of the research

This research is focused on the selection of fibre rich plant that is commonly found in Sri Lanka and to do the characterization of the fibres extracted to make conclusions on the possibility of manufacturing biodegradable textile material. Hence the *Lasia spinosa* (L.) Thwaites plant is selected as it is known as a rich source of fibres with medicinal values.

1.4 Research questions

- How to extract the fibres from rhizomes?
- What are the fibre characterization tools and methods?
- How to organize the fibre characterization tools and methods investigate fibre characteristics?
- How do the possibility of using *Lasia spinosa* rhizome fibre for manufacturing of biodegradable textile be explained?

1.5 Objectives

- To investigate possible fiber extraction mechanism.
- To identify fiber characterization tools and methods to characterize the extracted fibers.
-To investigate characteristics of *Lasia spinosa* rhizome fibre.
- To investigate the possibility of conversion of extracted fibers into a textile product and investigate properties

CHAPTER 2: LITERATURE REVIEW

2.1 Textile fibres

Use of fibres in textiles and clothing manufacturing begins from the development of human evolution and all the source of fibre is from nature until the industrial revolution. Hemp, flax, cotton and silk are such natural fibres obtained from plant and animal sources. During the period of the industrial revolution, between 18^{th} and 19^{th} centuries, new inventions of machineries took place in fibre processing and application. As a result, regenerated fibres like rayon and synthetic fibres like nylon and polyester were introduced to the textile industry [4].

The textile industry developed many types of commercially important synthetic polymers with considerable technological advances after the commercialization of regenerated fibres. Emergence of first synthetic polymers, nylon and polyesters, influenced bulk production of many other synthetic fibres, with very high technical specifications [5].

2.2 Natural fibre sources

Investigations on several different plant fibres are done by researchers with the intension of finding solutions to overcome these sustainability challenges facing by the textile industry. Cotton is the most abundant plant fibre in the nature. Flax, Jute, Ramie, Sisal and Abaca are known from ages as natural fibre sources. Lotus fibre, banana fibre, bamboo fibre, pineapple fibre and many other plant fibres have also been investigated by many researchers for textile applications.

2.3 Cellulosic fibres

Figure 2.1 presents the hierarchical structure of the cellulosic fibre found in nature. A number of small molecules connect together and make long chain molecules. Cellulose polymer chains together make microfibrils of 3-50 nm / 0.003 - 0.05 μm with crystalline phases and amorphous regions. Units of molecular chains lie parallel and compact adequately to make crystalline phases and randomly arranged at amorphous regions. Bundles of microfibrils together make macrofibre with diameter of 5-20 μm and macrofibres bundling makes cellulosic fibres [6],[7].

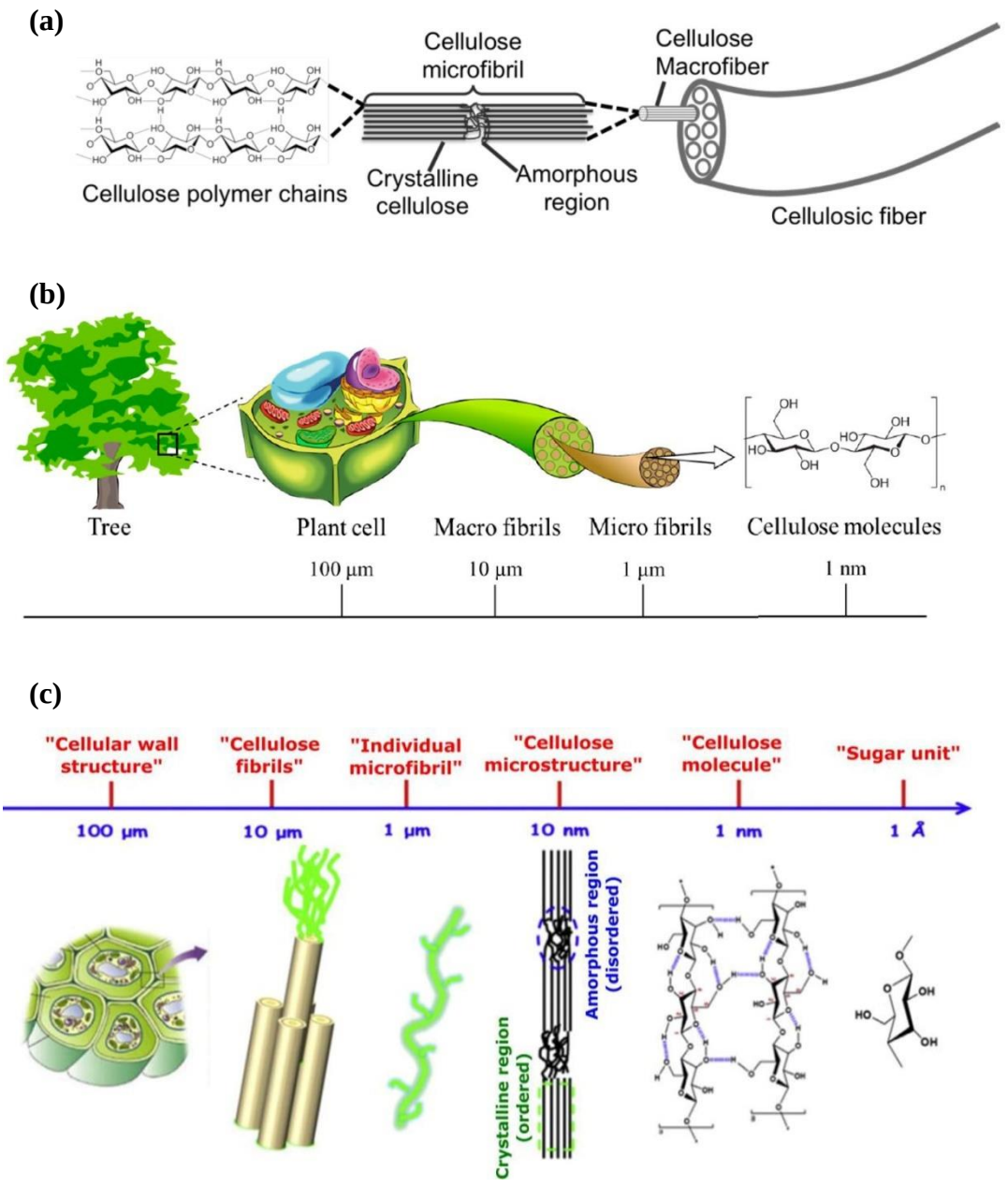

Figure 2.1: Hierarchical structure of cellulose fibres (a) - [6], (b) – [8], (c) – [9]

Several recent studies [8], [9] have recorded that the cellulosic fibres are formed with macro fibrils or fibrils that are with diameters of 10 µm, microfibrils of 1 µm and cellulose molecules of 1 nm.

These findings reflect that the researchers have explained the hierarchical structure of cellulose fibres based on the diameter of each stage. Diameter less than 1 μm are named as microfibrils. Terminologies of macrofibre, macrofibril and fibril are used by different researchers to define the stage with the diameter of 1 μm – 20 μm. Diameter above 20 μm is cellulosic fibre.

2.4 *Lasia spinosa* (L.) Thwaites

In the Sri Lankan context, *Lasia spinosa* (L.) Thwaites [LS] is a fibre rich source that is commonly used by Sri Lankans as a food due to its well-known medicinal values. When considering the historical records, it is understood that the LS plant is used for several medications from a long period of time. People have given a commercial value for this species as their stems, young leaves and rhizomes are used widely as a food. This plant is recognized as a herbal plant in Ayurvedic medicine of Sri Lanka and considered item as a plant that has the potential to use for variety of disorders such as anti-inflammatory, anti-helminthic, anti-diabetic, anti-bacterial, anti-oxidant, anti-hyperlipidemia, anti-tumor and with various other disease preventive factors [10].

LS species is distributed in Southeast Asian countries and it belongs to the family of Araceae. Rhizomes, leaves and stems of LS are a rich source of dietary fibres and as of that the pharmacological values of LS plant have been provided by many researchers according to Kankanamge [10], but proper scientific research evidences are not found on fibre characterization of the species with the scope of developing textiles.

As per the findings of the research, done by Tharanga [11], LS plants are categorized according to the leaf shapes of the species. Lamina-dissected [LD] type, Sagittate [SG] type, Mixed type and Black *Lasia* are the four main types. However, the LD type and SG type are comparatively common in most of the marshy lands in Sri Lanka than other two types. Leaf shapes mixed type is rarely found in Sri Lanka. It is assumed that the mixed type as an amalgamated plant of both LD type and SG type. According to the respective research findings, the Black Lasia is originated in Solomon Islands and it is an introduced species to Sri Lanka.

Usually LS is denoted by its plenty of sharp spines on its leaves, stems and rhizomes. Spineless type of LS can be found from few home gardens in the western and down south areas of Sri Lanka. This type belongs to the SG type. Though the spines are not available on their rhizome, they are slightly available underside of the leaves and leaf stems. Considering the presence or absence of spines in the LS rhizomes, these species are again clustered into three types, such as rhizome with high density of spines, rhizome with medium density of spines and rhizome with no spines [11].

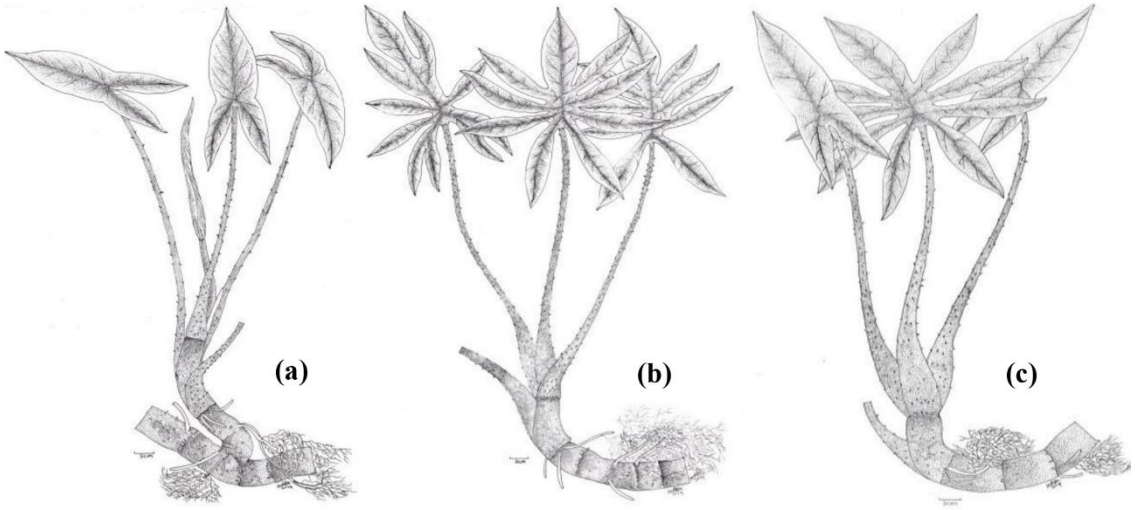

Figure 2.2: Morphological types based on leaf shape a: SG type. b: LD type. c: Mixed type [11]

Figure 2.3: Morphological types based on spines density a: Rhizome with high density of spines. b: Rhizome with medium density of spines. c: Rhizome with no spines [11]

Several studies [12], [13] have reported that the LS plants belong to the monocotyledonous plant group and are with fibrous root system. Anatomy of monocot root is shown in Figure 1.4 (a) [14] with scattered fibrous vascular bundles. Image (b) of the Figure 2.4 [14] emphasize the fibrous vascular bundles that are running down through the stem which continues in to the rhizome as well. Vascular bundle unit consists with xylem, phloem and bundle of fibres as in image (c) of the Figure 2.4 [15].

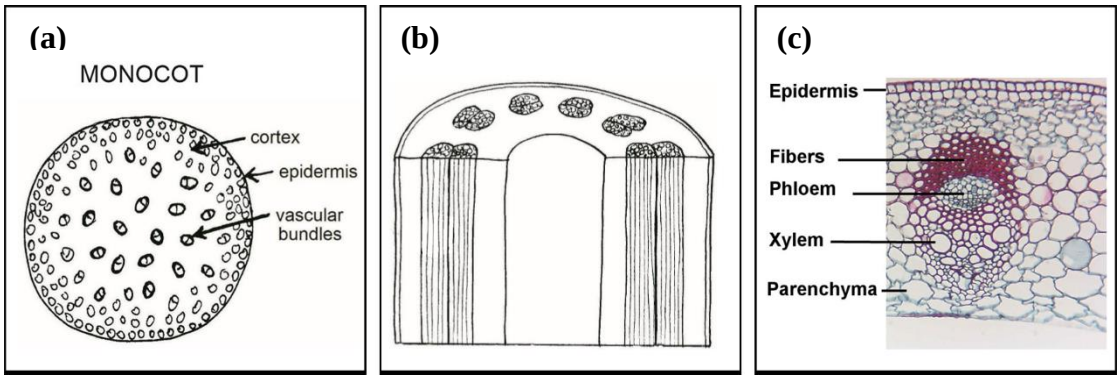

Figure 2.4: Monocotyledonous plant rhizome anatomy (a) cross section [14], (b) stem longitudinal section [14], (c) Fibrous vascular bundle [15]

Studies done by Baessler [16] have established that the rhizome is a continuation of the stem that grows horizontally just under the soil surface. Therefore, the anatomy of the rhizome expected to be as same as in the stems of the regular monocotyledonous plant.

2.5 Fibre characterization tools

In fibre characterization, it is required to investigate the surface morphology, chemical composition, structure, the crystalline and amorphous structure and some physical properties such as tensile strength, moisture absorbency and dye uptake of fibres. There are several instruments involved with the required investigations with their own unique principles in fibre characterization.

According to Mishara [4], it is essential to know the structure of the fibre, the raw material as well as the structure developed during processing so that the end-use properties can be controlled or modified for the specified applications. So, the analysis of the structure, as well as the structural measurements is essential for understanding the relationship the structure and quality of the end product. A complete understanding of the fibre structure requires investigations on its structural features like configuration, conformations, crystal structure and dimensions of crystallites, their arrangement, crystallite and crystallinity relationship and the nature of non-crystalline regions.

2.5.1 Scanning Electron Microscopy (SEM)

Scanning Electron Microscopy (SEM) is used exclusively for the examination of surfaces of materials, particles and fibres. SEM provides the requisite magnification suitable for the observation of fine details of the fibres via images. Clear understanding about the fibre surface characteristics, size of the fibres, fibrils and also the contaminants and their distribution and fibre cross sectional views can be viewed by the SEM under higher magnifications. Fine fibre structures and their diameters can be identified easily. The magnification is usually 10 to 100,000 times, depending upon the scanned sample surface. The size of the scanned area determines the magnification of the image. SEM has the ability to illustrate mass samples and three-dimensional views of fibres with in-depth view. An electron beam scans across the specimen in a series of parallel lines and high

vacuum is used in image producing of the SEM. Replica technique is used to avoid the instability of the material to high vacuum. It is necessary to coat the samples with chromium or carbon to provide a degree of electrical conductivity. In order to accomplish this, a chromium coater or a carbon coater is used [4]. According to the research done by Babu.et.al [17] in cotton fibre characterization, gold layer was sputtered on fibres before the SEM imaging. Hence either a gold coating or chromium or carbon coating to be sputtered on fibre samples prior to the SEM observation.

2.5.2 Fourier Transform Infrared Spectroscopy (FTIR)

According to Mishra [4], Fourier Transform Infrared Spectroscopy (FTIR) is used to do quantitative and qualitative analysis of polymer system by data processing system. FTIR provided spectroscopic information for structural analysis. The samples required for FTIR spectroscopy should be very thin and it should be either in the form of films, paste, disc, and solution, microtome or parallel arrangement of single filaments. Care should be taken in sample preparation to ensure high transmittance and better peak resolution for structural analysis.

FTIR spectroscopy method is a suitable tool to explore the hydrogen bonds that are existing within and in between the cellulose molecules in fibres. Further the identification of various bonds and the chemical constituents presented in the material along with the molecular structure can be done with this method. Standard KBr pellet technique is used to obtain clear spectrums from FTIR tests [18]. In accordance to the brief review done by Shaikh & Agrawal [19] on characterization of textile material by FTIR, it is identified that each IR absorption band in the spectrum represents the stretching or bending mode of the chemical bonds that are in the molecules after the absorption of IR radiations. Most considerable motions of the bonds within the molecules are bending and stretching. Wagging, rocking and scissoring are some of the other types of motions happen in the chemical bonds, once absorb the radiations. Stretching and bending requires a specific infrared weave. Bonded atoms of a molecule have its own arrangement which is unique to them. Due to this, the infrared frequencies absorbed by them are different to each other.

If the frequency of the light is exactly the same as the natural frequency at which the molecule vibrates, then the light will be absorbed by the chemical bond.

According to Shaikh.et.al [19] findings, the FTIR spectroscopy is split into two regions, group frequency region and fingerprint region. The wave number range of 400-1500 cm^{-1} belongs to the group frequency region and 1500-4000 cm^{-1}belongs to the fingerprint region. Group frequency region reflects the presence of chemical groups while the finger print region indicates the chemical compounds in the material.

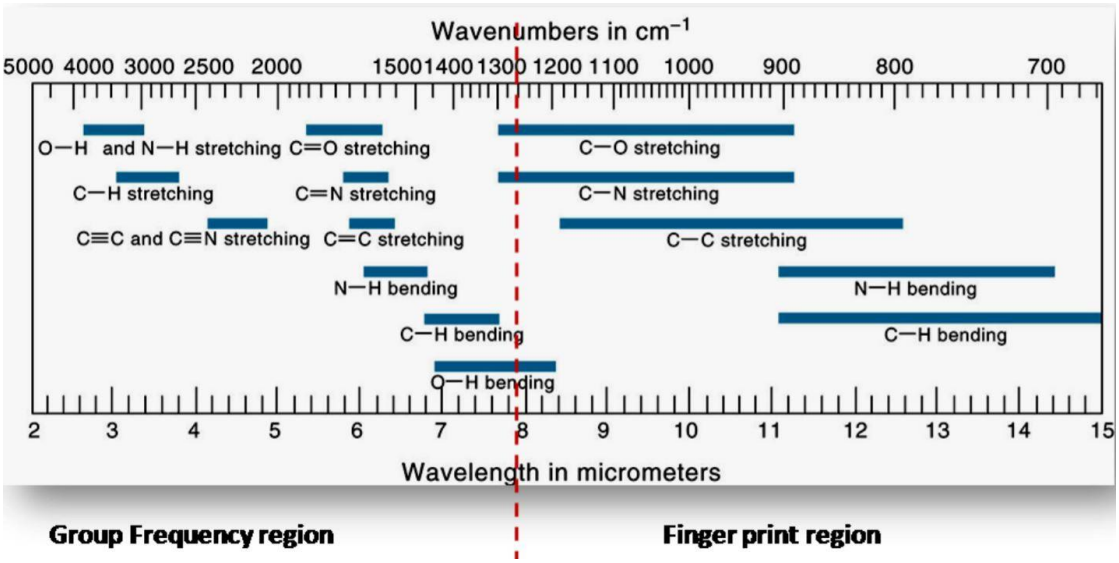

Figure 2.5: IR Spectroscopy Group frequency region & Finger print region [19]

2.5.3 X-Ray Difractometer [XRD]

X-Ray Diffractometer method is the most important technique to detect the types of crystals and crystallinity. As stated by Mishra [4], diffraction methods provide comprehensive information to draw conclusions of the single polymer chain, its direction and partnering with neighboring polymer chain. Further a qualitative and quantitative calculation of the crystalline components in the semi-crystalline polymers such as cellulosic fibres can be performed. Crystallinity measurement from IR spectroscopy offers the advantages for a complete understanding of the microstructure of the fibre in terms of crystal structure, chain folding, arrangement of crystallite and the nature of non-crystalline

regions. In another point of view, the XRD features degree of crystallinity, microstructure, indexing of crystal structure, orientation, which are important in polymer or fibre analysis.

2.5.4 Thermogravimetric analysis

Thermal stability is an important characteristic to investigate in deciding the suitability of the fibre for high temperatures applied during manufacturing processes. Thermal stability and the thermal decomposition of natural fibres can be evaluated by the Thermogravimetric analysis [20]. According to several research reviews, weight loss of the fibre sample is measured as a function of temperature and time [22],[26], [38], [39].

2.5.5 Tensile behavior

Tensile behavior of natural fibres is an important characteristic to determine its mechanical performance. Instron universal tester was used by several researches [21],[22] with 50kN load capacity to investigate the tensile properties of fibres. Fibre elongation at varying tensile loads was studied and the breaking strength and breaking elongation was calculated in those investigations to compare and conclude the tensile properties of the respective fibres.

2.5.6 Moisture absorbency

Determination of moisture absorbency properties of fibres is also found as an essential test to perform of the fibres in its characterization [23].

2.5.7 Dye-uptake behavior

Fibre dye-uptake behavior is an important characteristic of natural fibres and a colour spectrophotometer is used to measure it. Several recent studies [24],[25],[27] have recorded the use of spectrophotometer in measuring the dye-uptake of natural fibres. According to Shak Sadi and Jakir Hossain [24], shade, reflectance and colour strength (K/S) parameters are measured in characterizing the dye-uptake of dyed textile samples. Colour strength is determined calculating the percentage value of weight of dye applied on a certain weight of fibre. Shade influences the reflectance of the dyed textiles. Energy source and the energy detector in the spectrophotometer, measures the effectiveness in reflecting radiant energy and that is considered as reflectance of the material. Further it is

stated at the less energy absorbance, the reflectance is high and at the high energy absorbance the reflectance is less. Color strength (K/S) values should be found out to test the depth of dye absorbency as a quality measurement of a dyed fabric.

As per all the above information, it is shown these analytical tools could be used in characterizing LS rhizome fibre.

2.6 Fibre characteristics of Araceae family

Even though there are no research findings on characterization of LS fibre, there are fibre characterization studies done on the fibres belonging to the same plant family. LS is belonging to the Araceae plant family. *Epipremnum aureum* is a breed of blossoming plant in the same family, native in Mo'orea, Polynesia [26]. These plants that can be used to extract Bio-fibres are typically growing in wide range of climate conditions. Contained chemical components in cellulosic fibres are depending on growing area, condition of soil, maturity of the plant and extraction process. As per the results obtained from the FTIR spectroscopy of *Epipremnum aureum* fibres [EAF], they are consisting of functional groups of 61.34°wt% cellulose, 13.42°wt% hemicelluloses and lignin 14.01°wt%.

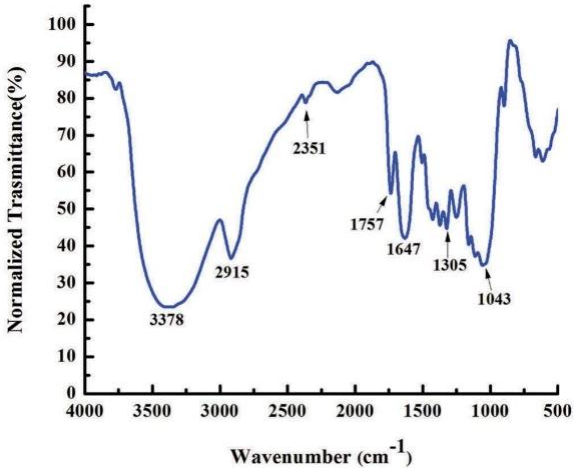

Figure 2.6: FTIR spectrum of the EAF [26]

The high lignin content is pointed out as the reason for the water to retain in the fibre and contributes to the fibre arrangement while helping to resist biological attacks. The EAF density is recorded as 654 kg/m3, and that is outstandingly less than the man-made fibres.

The researcher has concluded suggesting the EAFs for the development of light-weight composites [26].

According to the X-ray diffraction analysis of EAFs done by Maheshwaran et.al [26], it is confirmed that the crystallinity index of EAF is 49.33. According to Figure 2.7, the highest peak at $2\theta = 22.23°$ is attributed to the crystal phases of cellulose I and the intensity peak at $2\theta = 15.46°$ indicates the amorphous regions such as amorphous cellulose, hemicelluloses, pectin and lignin. The crystallite size was determined as 15nm.

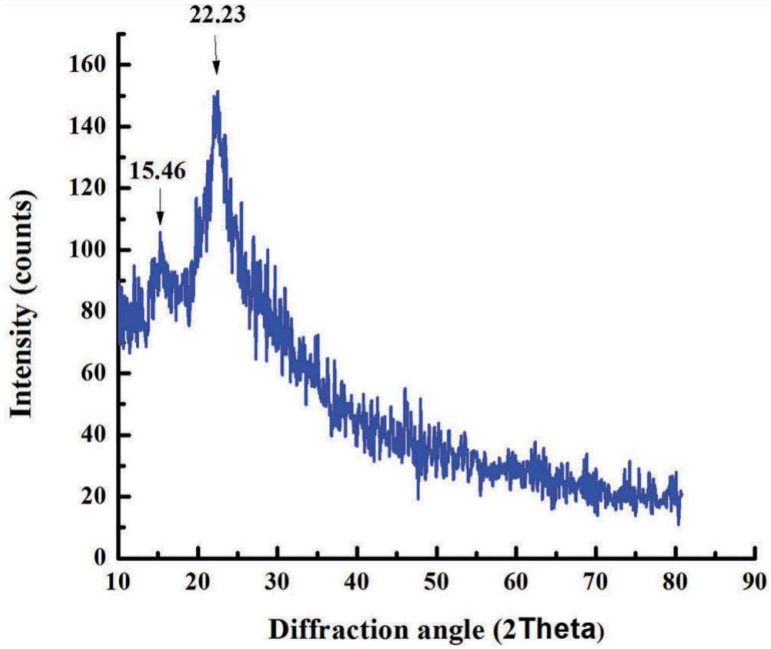

Figure 2.7: XRD spectrum of EAFs [18]

Through the scanning electron microscopy [SEM] images, it is witnessed the EAF have a rough surface with collected impurities on them. Hence it is suggested that these fibres are appropriate for bonding with polymers.

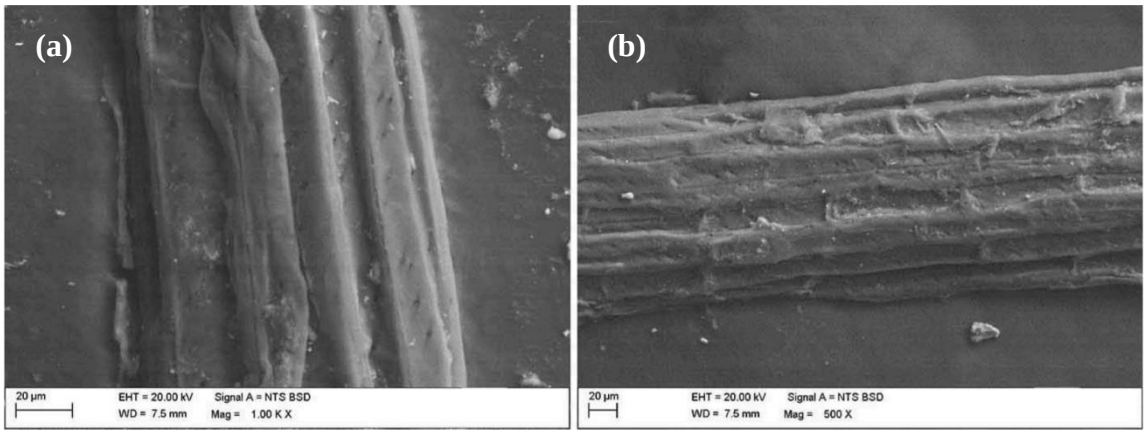

Figure 2.8: SEM observation of EAF [26]

With tensile strength results of EAF, it is suggested that the fibre is suitable to be used in the manufacturing of polymer composites with the synthetic fibres using the ability of reinforcement [26].

2.7 Cotton fibre characterization

In conventional cotton manufacturing, the cottons are grown by using synthetic fertilizers and pesticides. This has led for many environmental problems over the last few years. General increase in awareness of the sustainable issues resulted manufacturers to pay their attention on organic cotton productions with the use of organic farming methods and standards [17].

2.7.1 Cotton fibre morphology

A natural vegetable fibre, Cotton is the most use plant fibre in the world. Hence it was decided to find relevant research work on characterization of cotton fibre. Figure 2.9 (a) presents the linear helical shape which is similar to the shape of a ribbon [17] and the fibre cross section (b) looks like bean shape [20].

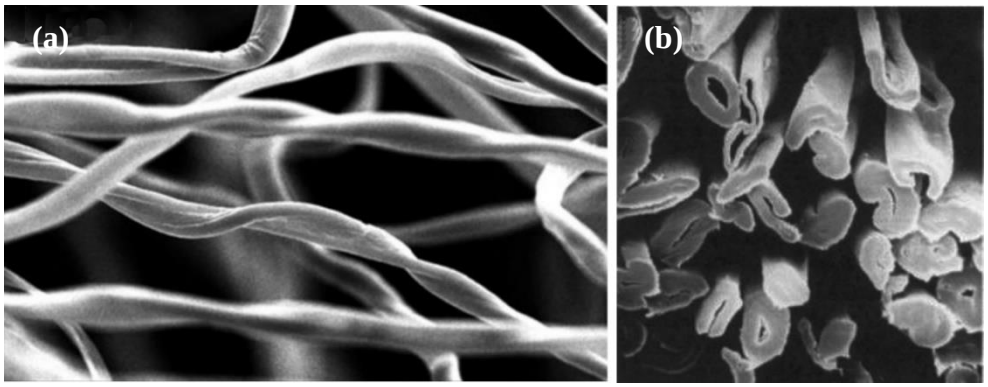

Figure 2.9: SEM image of the Cotton Fibre [17], [29]

The cotton fibre outer skin is consisting with randomly organized micro fibrils among a combination of proteins, pectin, waxes and some non-cellulosic components. As of those non-cellulosic components, the fibre surface appears as a non-fibrillar surface. Further these non-cellulosic components provide a lubricant surface for processing and the water repellent protection. Removal of the waxy component on the primary wall of the fibre makes it easier for the dye particles and other finishing chemicals to migrate into the fibre. Both the primary and the secondary walls are connected by a thin layer known as winding layer which consists of microfibril bands, lying inside the primary wall of the fibre as in Figure: 2.10 [a].

Secondary wall of the fibre is considered as the main body of the fibre. It is formed with spiral shaped parallelly laid fibril layers. Fibrils of the secondary wall which are closer to the primary wall of the fibre are formed nearly 45°angle towards the fibre length direction as in Figure: 2.10 (b). However, fibrils are parallel to the fibre axis at its core area as in Figure: 2.11 (a) & (b). It is considered that the fibrils that are compacted closely are formed with pure cellulose [30].

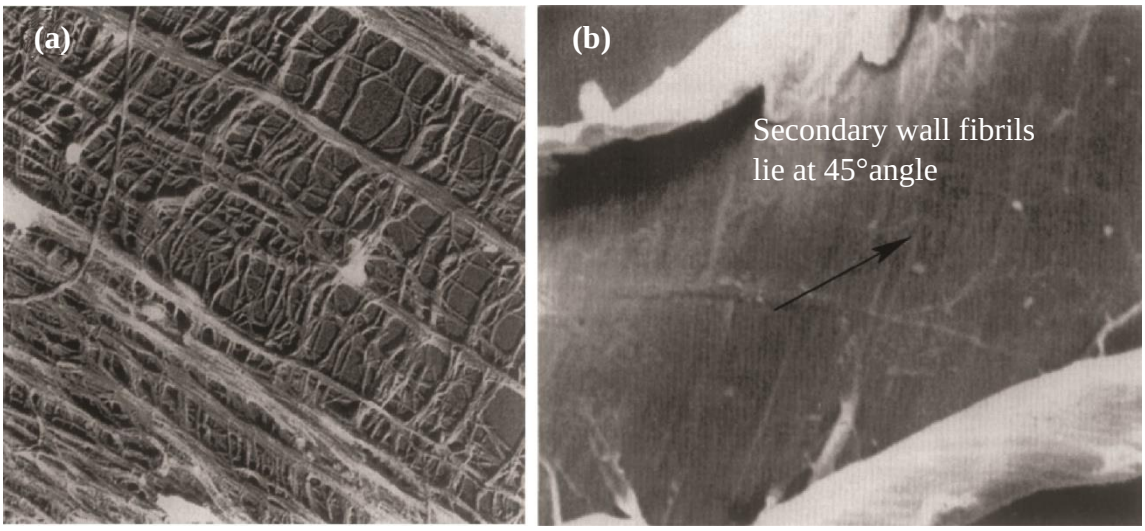

Figure 2.10: Cotton fibre Transmission Electron Microscopy [TEM] view (a) winding layer, (b) fibrils of the secondary wall nearer to primary wall formed at 45° to fibre axis (SEM) [30]

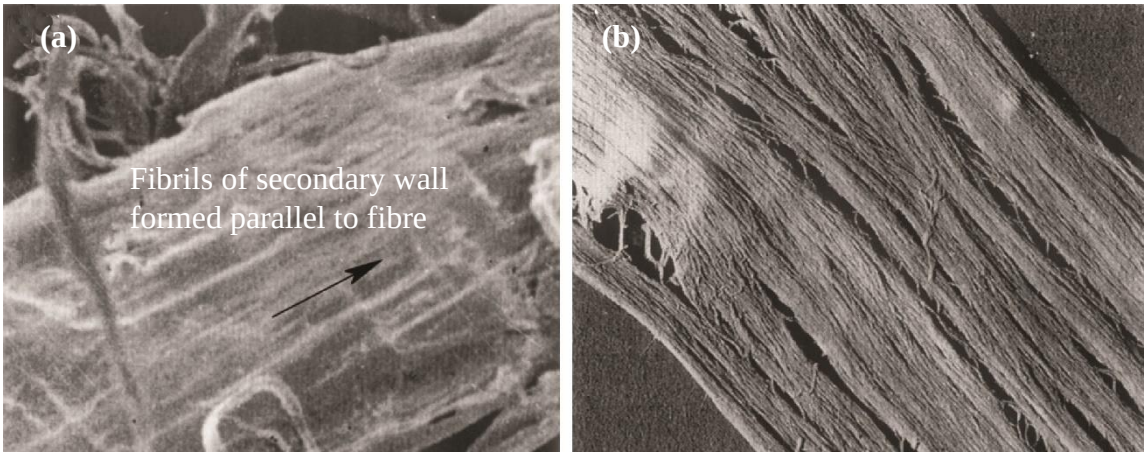

Figure 2.11: Cotton fibre fibril formation (a) parallel lying fibrils of secondary wall at fibre core area (SEM), (b) Microfibrils of secondary wall (TEM) [30]

Normally cellulose fibre wall component consists of fibrils which are less than 1 μm and microfibrils of 0.001 μm up to 0.1 μm. Structure of the microfibril is a blend of crystalline and amorphous phases. Generally, fibrils are known as building units of natural cellulose. It is found that the cotton, jute and ramie fibres are having biological structure similar to that of the wood fibre [31].

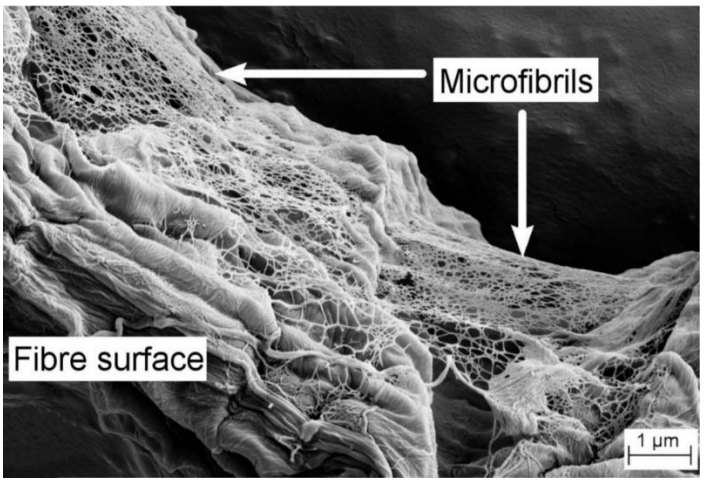

Figure 2.12: Micro fibrillated cellulose structure of wood fibre [31]

2.7.2 Chemical constituents in Cotton

Many researchers found the surface chemical composition and internal chemical composition of natural fibres through FTIR spectroscopy result analysis. All plant fibres are mainly composed with cellulose, hemicelluloses, pectin and lignin. Bound water, remaining proteins, waxes and some inorganic compounds are also found on fibres apart from the main elements. Cell walls are mainly composed with cellulose making crystalline phases by fibril structure mixing with amorphous phases. Cellulose microfibrils are surrounded with amorphous regions composed with hemicelluloses built with polysaccharides [22].

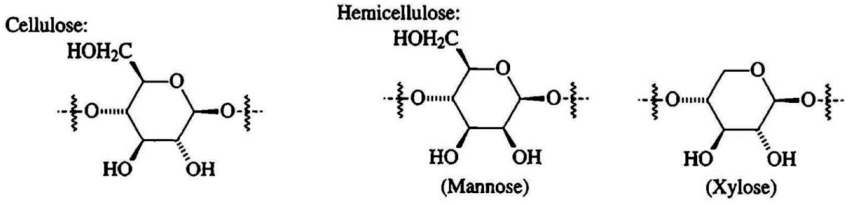

Figure 2.13: Structure of the Cellulose and Hemicellulose monomers [32]

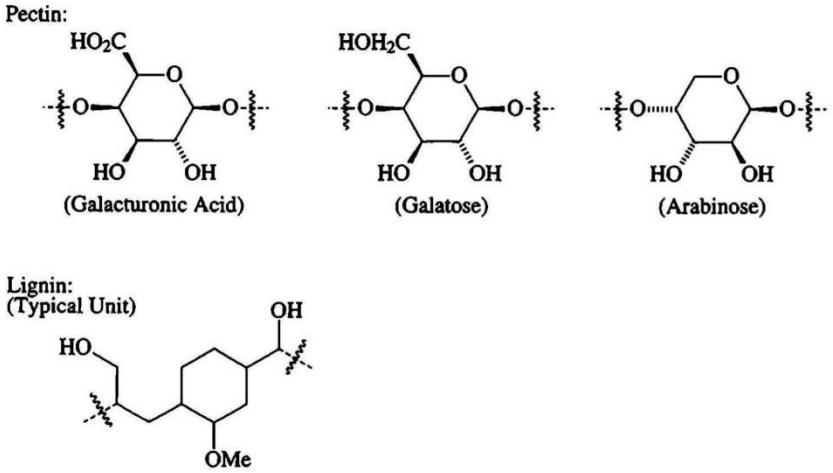

Figure 2.14: Structure of Pectin and Lignin monomers [32]

Pectins are polymers composed with galacturonic acid. Lignin is a polysaccharide formed with chains of glucose molecules. Structures of both lignin and pectin are shown in Figure 2.14 [32].

Presence of methylene (CH2) groups in fibres confirms by the peak values of 2918 cm^{-1} and 2849 cm^{-1}. These values are recorded due to the symmetric and asymmetric stretching of methylene (CH2) groups in alkyl chains of waxes. Scouring results, the removal of waxy layer from the surface. Hence the FTIR spectrum of scoured fibres shows lower intensity peaks at 2918 cm^{-1} and 2849 cm^{-1}, which was recorded with higher absorbency values at the un-scoured stage due to the presence of waxes on fibres [17].

Peaks attributed to the stretching of C=O, C–H and vibration of the bending of bound water are observed at weave numbers between 1500 cm^{-1} and 3000 cm^{-1}. Peaks for the stretching of O-H bonds presents in between the molecules and within the molecules were observed at the weave region of 3700–3000 cm^{-1}. Stretching of CH groups in cellulose indicate by the peak record at 2900 cm^{-1} [17].

FTIR curves obtained for the conventional and organic cotton fibres are shown in Figure 2.15. Shape of the two spectrums are similar to each other. However, it is evident that the intensity of transmission varies in the spectrums and more IR absorbance is observed by

the organic cotton than by the conventional cotton fibre. Researcher has concluded that this occurs due to the different proportions of component representation in each fibre [17].

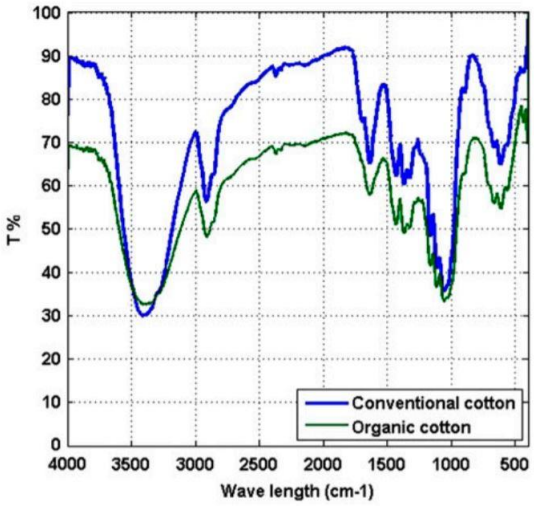

Figure 2.15: FTIR graphs of organic and conventional cotton fibres [17]

There are several studies [33],[34] about the chemical composition of cotton fibres. According to these studies, both the structure and composition of the cellulose and non-cellulosic constituents varied depending on the cotton variety, differences in maturity of fibres and the growing conditions. According to Paul [32], cotton fibres contained higher amounts of cellulose and several other non-cellulosic components. Constituents percentage values of cotton fibre presented by different researchers were observed to be within a narrow range. Therefore, a range value for each component can be suggested. Accordingly, cellulose 88.0% - 96.0% as the major component and hemicelluloses and pectin 0.7-1.2%, wax 0.4-1.0%, ash 0.7-1.6%, water 0.5-1.0% could be stated. In addition, very low amount of organic acids also could be found.

According to the cotton fibre study done by Liu [35], the crystallinity indexes (CI) of fine and coarse cotton fibres are reported as 71.7% and 70.0% respectively. However, according to Murugesh Babu [17], slightly different CI values of 63.59% and 63.41% were recorded for conventional raw cotton and organic raw cotton fibres respectively.

2.8 Natural fibre characterization

There is a significant number of research work on different other natural fibres carried out and published in different regions of the world. Some of the fibre sources are unique to certain regions such as lotus fibre which is widely spread in the Asian region. As stated in the lotus fibre studies [21],[36], [37] the morphological observation was carried out by SEM, TEM and Atomic Force Microscopy. It is observed that the researchers have carried out chemical nature determination by FTIR analysis, crystallinity parameter measurement by X-RD, properties such as moisture regain and tensile strength determination using oven dry method and tensile strength tester respectively.

2.8.1 Lotus fibre

2.8.1.1 Scanning electron microscopy analysis

Ritu Pandey et.al.[36] have observed natural crimp on lotus microfibres at the lotus fibre morphology investigation done by SEM. Narrowing and smooth ends were observed at the latter part of the fibres.

According to Dong-sheng Chen,et.al.[37], single fibres are closely formed beside each of them and appears with helical structure along the fibre axis as in (a), (b) and (c) images of the Figure 2.16. Cross section of the single fibres have a circular shape as shown in Figure 2.17.

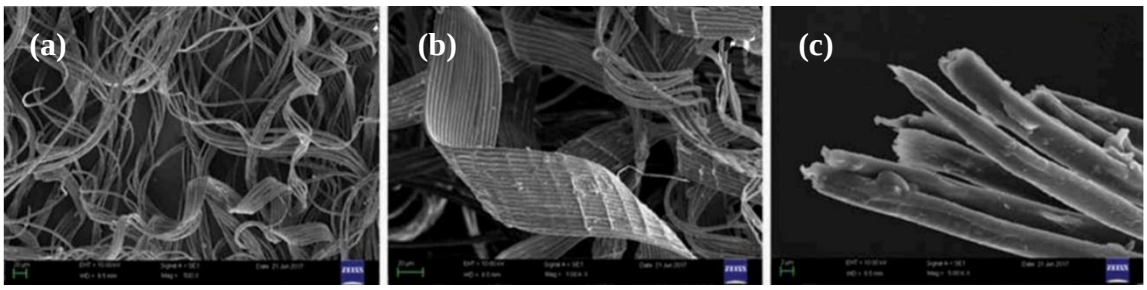

Figure 2.16: SEM images of lotus fibre (a), (b) spiral shape of fibres (c) fibres at increased magnification [36]

However, Cheng Cheng, et.al.[37] have observed an irregular shaped cross section on lotus fibres as in Figure 2.18. Further it is reported that the fibres are observed with 75 μm

- 80 µm diameter together with grooves running along the vertical axis of them. Non-cellulosic compounds, pectin and waxes are contaminated on the surface of mechanically extracted lotus fibres. The raw lotus fibres observed by the naked eye consist of fibre bundles, which are connected by non-cellulose substances. Lotus fibres are somewhat like hollow fibres that are fine in its structure and covered with an external covering.

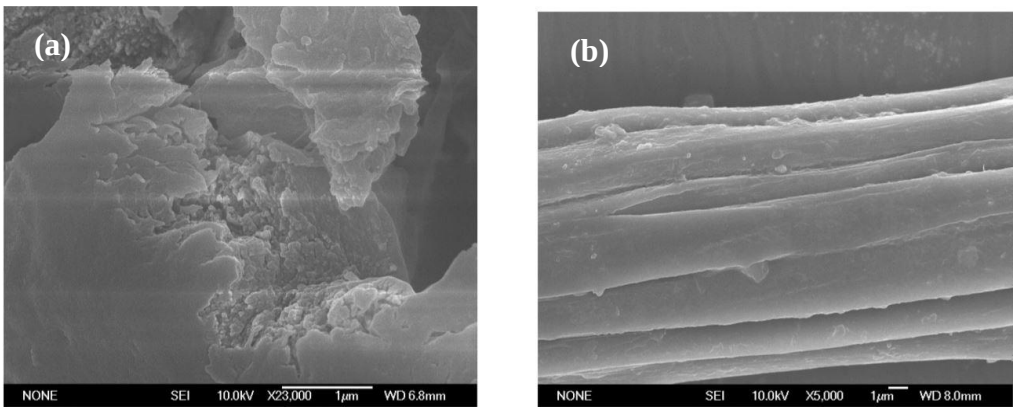

Figure 2.17: Lotus monofilament fibre (a) cross section (b) longitudinal section [37]

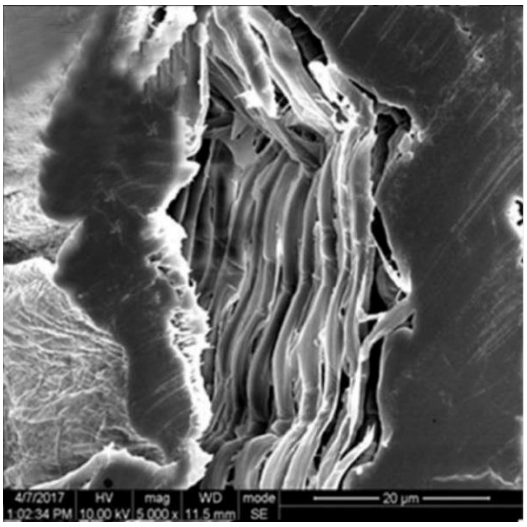

Figure 2.18: Irregular cross-sectional shapes of lotus fibres [40]

According to the findings of both the above research works [37], [40], it is obvious that the lotus fibre cross section is more or less circular in shape, but has a wrinkled surface.

A rough surface with lengthwise grooves of different depths was observed by Ying Pan, et.al.[21] in their study on the characterization of the surface microstructure of the lotus fibre by using Atomic Force Microscopy (AFM). Bundle like combined fibrils which are arranged parallel with diameters ranging 30nm – 100nm were recorded under further observations. Combined fibrils appear as disordered formations in certain areas of the fibre making the surface of the fibre uneven. Such uneven surfaces are formed by unequally lifted up formations leading to high level of coarseness. In certain areas, the fibrils are formed parallel to each other and those areas are characterized by relatively lower level of milled roughness. These uneven surfaces make it easier for the moisture and chemicals to absorb into the fibre.

2.8.1.2 FTIR analysis

FTIR spectrums recorded in lotus fibre investigations [36], [38] clearly indicating that the lotus fibre follows similar spectra to the cotton fibre spectra [17], [28]. According to Ritu Pandey, et.al.[36], the peak obtained at 1034 cm^{-1} and as per Dong-sheng Chen, et.al.[37], the peak obtained at 1052.4 cm^{-1} are representing the vibration occurs at stretching of C–O bonds in fibres. However, intensity of stretching of C-O bonds in cotton fibre is more visible than in the case of lotus fibre. Lower peak value at 1034 cm^{-1} suggests a lower amount of availability of C-O bonds in lotus fibre. According to Ritu Pandey, et.al.[36], peak observed at 1241 cm−1 in cotton fibre was suggested as due to the stretching of C-H bonds. The 1241 cm−1 peak was not observed on FTIR spectrums of lotus fiber investigations. The peak value of 1249.9 cm−1 observed in the lotus fibre research done by Dong-sheng Chen, et.al.[37] was interpreted as due to the vibration of C-O bonds in hemicelluloses and Galactans. Broader peaks at 3348 cm−1 and 3354.4 cm−1 were recorded in two investigations [36], [37] and it was stated that they occur due to the OH stretching of the molecules. By analyzing the FTIR data recorded in afore mentioned researchers, it is understood that the chemical nature of both cotton and lotus fibre are similar, but the number of chemical compounds and their compositions differ.

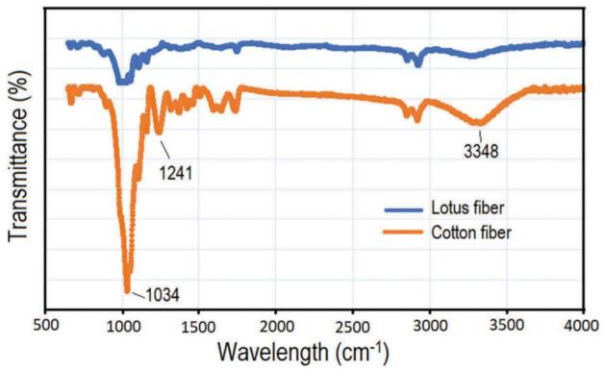

Figure 2.19: FTIR graph of cotton and Lotus fiber [36]

FTIR analysis done by Ying Pan. et.al [21] on lotus fibre has confirmed that the fibres are generally developed with cellulose, hemicelluloses, and lignin. As recorded, the content values of cellulose, hemicelluloses, and lignin are 41.4 ± 0.29%, 25.87 ± 0.64%, and 19.56 ± 0.32%, respectively. In comparison with other cellulosic fibres, it is found that the lotus fibres have a high amount of contamination percentage of hemicelluloses and lignin. Results obtained by Dong-sheng Chen.et.al [37] during his study of the chemical compounds in natural fibres are presented in Table 2.1.

Table 2.1: Presence of different chemical compounds in natural fibres (%) [37]

Fibre type	**Cellulose**	**Hemicellulose**	**Lignin**	**Pectin**	**Fat waxy**	**Ash**
Lotus	68.04	9.36	8.76	3.2	3.1	2.9
Cotton	90 – 95	1.1 – 1.9	-	0.3 – 0.8	0.6 – 0.9	0.8 – 1.3
Ramie	65 – 75	14 – 16	0.8 – 1.5	4 – 5	0.5 – 1	2 – 5
Flax	70 – 80	12 – 15	2.5 – 5	1.4 – 5.7	1.2 – 1.8	0.8 – 1.3
Jute	64 – 67	16 – 19	11 – 15	1.1 – 1.3	0.3 – 0.7	0.6 – 1.7
Bamboo	44 - 53	19 - 25	23 - 33	0.6 – 0.9	-	1 – 1.9

According to the above results, the amount of cellulose in lotus fibre is lower than that in cotton and flax fibres. Cellulose percentage in lotus fibre is higher than that in jute and bamboo fibres and it is similar to the amount in ramie fibre. In lotus fibres, the presence

of hemicelluloses, pectin, waxy compounds and ashes are found to be higher than in cotton, bamboo and flax fibres. High percentage of lignin is presented than cotton, flax and ramie fibres. However, the lignin percentage in lotus fibre is less than the bamboo and jute fibres. These results prove that the cellulose is the most presented chemical compounds in plant fibres. According to the percentage values of different compounds mentioned in table 2.1, it is understood that the lotus fibres are consisting with high percentage of impurities than other plant fibres. According to the researchers, it is required to remove those impurities stagnated on fibres to remove the dye matter and to improve the absorbency of dyes in fibre processing.

2.8.1.3 Crystallinity Index

In their study of lotus fibre, Dong-sheng Chen.et.al[37] investigated further about the crystal structure such as crystallinity index [CI], percentage of crystalinity [%Cr], crystal size [CS] and the direction of crytals positioning by X-Ray diffraction method and the results comparison with cotton fibre.

Table 2.2: Comparison of CI and percentatge crystallinity of lotus and cotton fibres [21]

	Lotus fibre	**Cotton fibre**
Crystallinity %	48%	65%
CI	52	60

As per the above values, it is evident that the lotus fibre CI and percentage of crystallinity are lower than those of cotton fibres. Fibres with a low degree of crystallinity has less crystal regions but high amorphous regions. As of this structure, the lotus fibre is having greater hygroscopicity and chemical reactivity but lower in strength. High ctrystalite orientation and CI reflects high srength but lesser elongation. CS of the cotton and lotus fibres were found as 6.1 nm and 2.5nm respectively. Compared to cotton fibre, it is understood that the lotus fibre is having low CS. Fibres with low CS's makes larger surface area on it. Hence those fibres were observed with high moisture and chemical absorption properties [21].

Cotton fibre X-Ray diffraction pattern obtained by Teixeira, et al. [29] is shown in Figure 2.20. This diffraction pattern indicates the main peak of the cotton fibre around 2θ = 22.6°.

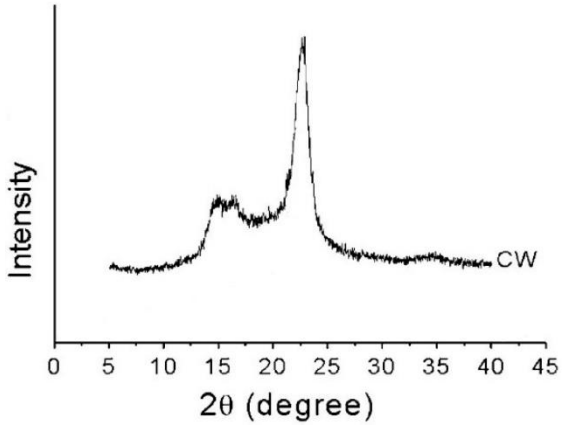

Figure 2.20: X-Ray diffraction pattern of cotton fibre

Many recent studies [20], [22], [38] have recommended to use the following equations to calculate the crystallinity index of the fibres.

Equation 1

$$\mathrm{CrI\%} = \left(\frac{I_{002} - I_{am}}{I_{002}}\right)^{0} X\ 100$$

Equation 2

$$\mathrm{CI} = \left(1 - \frac{I_{002}}{I_{am}}\right)^{0} X\ 100\ \%$$

The peak intensity, I_{002} which the crystalline phase at 2θ of the lattice diffraction for cellulose I and I_{am}, the lowest intensity for the amorphous region at 2θ were obtained from the diffraction pattern to calculate the CI.

Further the above researchers have applied the Scherrer's equation to calculate the CS of the respective fires using the following equation.

Equation 3

$$Cr_{size} = \frac{K\lambda}{\beta\ Cos\theta}$$

Scherrer's constant (K) = 0.9, weave length of the radiation λ = 1.54 Å [0.154 nm] and β the peak's full width at half maximum [FWHM] while θ is the diffraction angle are input

to the equation to calculate the size of the ordered domain which is the crystalline phase size. The researcher has calculated the maximum width at half the maximum intensity as in Figure 2.21[4].

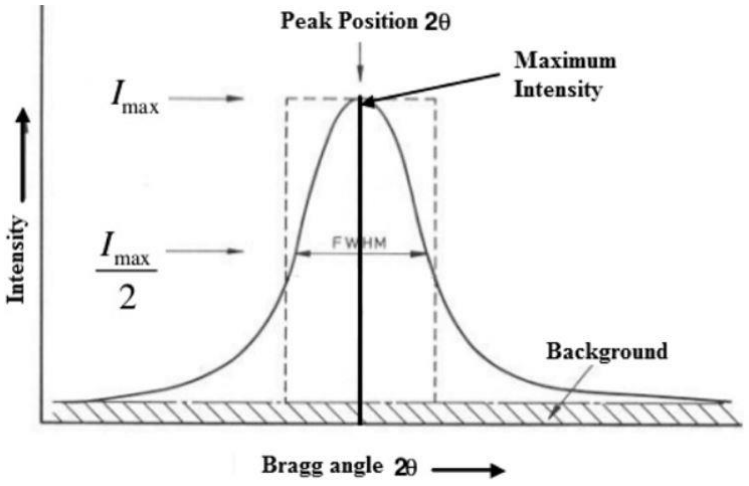

Figure 2.21: FWHM in X-Ray diffraction pattern [4]

2.8.1.4 Tensile behaviour

Tensile behaviour of fibres is an important characteristic to be investigated. Several researchers [21],[26],[29],[36],[38] have tested the tensile behaviour of the different cellulosic fibres.. According to [21], the lotus fibre tensile strength is 2.23 cN/dtex, Young's modulus is 78.5cN /dtex and the breaking elongation is 2.6%. However according to Ritu Pandey et.al.[36], lotus fibre elongation is 1.95%, mean fibre tenacity is 13.41g/tex and the average breaking strength is 3.06g. The difference between the fibre elongation of the above two research findings is 0.65 and that may occur due to many reasons such as different growing conditions, fibre samples of different maturity level or the variations in testing conditions and equipment. Table 2.3 shows the tensile behavior of well-known fibres from several plants [22] and recently investigated fibres by different researchers [26], [38].

Table 2.3: Tensile behaviour of natural cellulosic fibres [22],[31],[38],[41]

Fibre Type	**Elongation at break %**	**Tensile strength (MPa)**	**Young's Modulus (GPa)**
Cotton	7 – 8	400	5 – 12
Flax	2.07 – 0.45	945 ± 200	52.5 ± 8.6
Jute	1.15 – 1.5	340 - 470	1.3 – 42.2
Hemp	2.2	285	14.4
Ramie	2 - 3	220 – 938	44 – 128
Sisal	2 - 2.5	511 – 635	9 - 22
Banana	1- 3.5	529 – 759	8
Pineapple	2.2	126.6	4.405
Bamboo	1.4	503	35.91
Coccinia grandis L.	2.703 ± 0.273	273 ± 27.74	10.17± 1.261
Epipremnum aureum	1.38 – 4.2	317–810	8.41– 69.61
Althaea officinalis L.	3.9	415.2	65.4
Cissus quadrangularis	3.57 – 8.37	1857 – 5330	68 - 203

2.9 Different fibre extraction methods and fibre characterization

Several researchers [21],[38],[39],[42] have carried out investigations of different fibre extraction methods of natural fibre sources. Those researchers have proved that the extraction method has an effect on fibre properties. According to those researchers, mechanical–extraction, water extraction and alkali extraction methods were applied in extracting fibres from plant sources.

According to literature findings, both water and chemicals are used to extract fibres from the stems of Althea officinalis L. [32]. NaOH is used for chemical extraction. Researcher has observed that the peaks corresponds to the hemicellulose and lignin are reduced or completely disappeared in the spectrum of FTIR of the NaOH extracted fibres because of

the compositional changes due to NaOH when the fibres are boiled. Improvement in crystallinity index by NaOH boiling is proved by the X-RD results. Crystallinity index of water extracted and alkali extracted were determined as 65% and 74% respectively. A tensile strength of 200 ± 58 MPa has been recorded for water extracted fibres and 274 ± 26 MPa for NaOH extracted fibres. All the above results show that the fibre extraction by boiling for 2 hours in 5% NaOH solution, is a better method than extracting fibre with water retting method.

As per the investigation done by Senthamarikannan [38], in characterizing cellulosic fibre from *Coccinia grandis L.* stems, raw fibres were dipped in 5% NaOH for 45min at room temperature and then were dipped in 1% HCl solution for 1min and then washed and dried in the air oven at 80 ℃ for 6 hours. Fibres extracted from different extraction methods were observed with clear differences in ther morphology. Untreated fibre surface was observed with rough and uneven textures as of the presence of wax, pectin, lignin, oil and impurities on the surface. The alkali extraction method improves the surface roughness of the fibres due to the removal of pectin, lignin, oil and impurities on the surfaces. The SEM observations of the alkali extracted and water extracted *Coccinia grandis L.* fibre are presented in Figure 2.22.

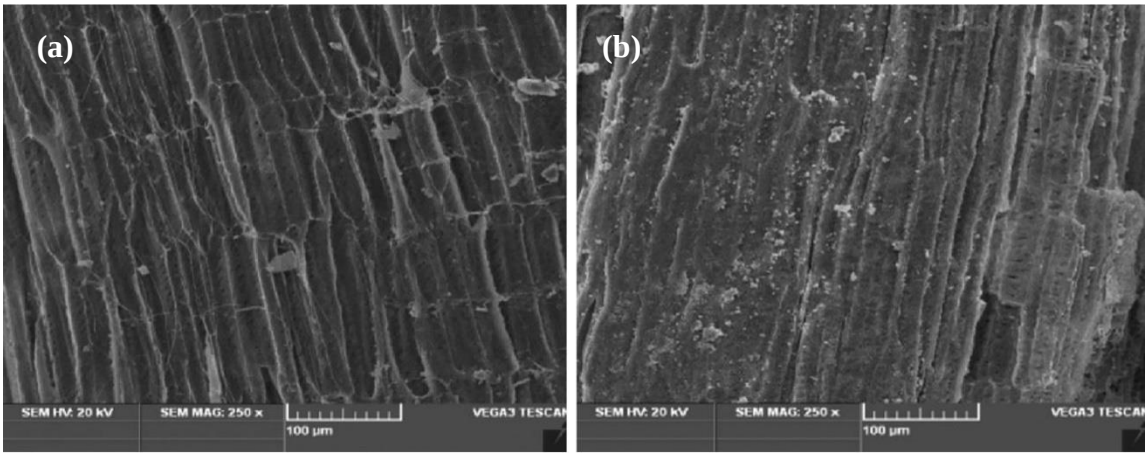

Figure 2.22: SEM image of *Coccinia grandis* L. fibre (a) water extracted fibres, (b) alkali extracted fibres [38]

Measures of the fibre properties of *Coccinia grandis L.* fibres due to the effect of extraction methods are presented in below table.

Table 2.4: Fibre properties of water and alkali extraction *Coccinia grandis*. *L* fibre [38]

Fibre property	**Water extracted fibre**	**Alkali extracted fibre**
Fibre diameter	27.33 ± 0.3789 μm	25.48 ± 0.3014 μm
Tensile strength	273 ± 27.74 MPa	316.3 ± 36.63 MPa
Moisture Content	5.6%	4.8%
Elongation at break	2.703 ± 0.2736 %	2.258 ± 0.2834 %
Crystallinity index	52.17%	57.64%

As per the table 2.4, it is identified that the fibre diameter, moisture content and elongation at break have decreased when treated with alkali while showing an increase in tensile strength and the crystallinity index.

According to Ying Pan et al. [21], mechanical extraction method was followed in extracting fibres from lotus stems. Cheng Cheng et al. [23] has followed chemical extraction through treatment of NaOH with sodium chlorite to extract the fibres from lotus stems. Fibre property results of both the investigations are mentioned in the table 2.5.

Table 2.5: Mechanically alkali extracted lotus fibre properties

Fibre Property	**Mechanically extracted Lotus fibre [21]**	**Alkali extracted Lotus fibre [23]**
Tensile Strength	5.25 cN/dtex	1.4 cN/dtex
Moisture regain	12.3%	4.34%
Elongation at break	4.07%	3.6%
Crystallinity Index	52%	62.29%

Fibres extracted using two different chemical formulae were compared by Cheng et al. [23]. Therefore, it is difficult to compare those results with the characterization results of mechanically extracted fibres from lotus stems done by Ying Pan et al. [21]. However, it is proved that the chemically extracted fibres showed a clear decrease in the tensile strength, breaking elongation and moisture regain of fibres while showing an increase in crystallinity index.

Several researchers have investigated the thermal stability of the plant fibres to identify thermal stability of respective fibres [26], [39], [22].[38]. According to the fibre type it is identified that the thermal degradation happens in different phases. Table 2.6 shows the results of the thermogravimetric analysis of few different fibres extracted by the water retting process.

Table 2.6: Thermal stability of natural fibres

Fibre	**Thermal Degradation**		**Reference**
	Temperature Range	**Reason**	
Epipremnum aureum	Room temperature – 100℃	Evaporation of moisture	Maheshwaran [26]
	240℃	Degradation of hemicelluloses	
	240℃ - 380℃	Degradation of celluloses	
	380℃ - 600℃	Thermal depolymerization of wax	
Althea officinalis L.	45℃ - 110℃	Evaporation of water	KılınÇ et al. [39]
	190℃ - 310℃	Decomposition of hemicelluloses and glycosidic linkages of cellulose	
	310℃ - 370℃	Decomposition of cellulose I and ∝-cellulose	
Coccinia grandis L.	213.4℃ - 296.17℃	Degradation of hemicelluloses,	Senthamaraikan[38]

Fibre	Thermal Degradation		Reference
	Temperature Range	**Reason**	
		lignin and glycosidic bonds of cellulose	Senthamaraikan[38]
	296.17℃ - 351.6℃	Cellulose degradation	
	351.6℃ - 520.16℃	Degradation of wax	
Cissus quadrangularis	89℃	Removal of moisture from fibre	S. Indran et al. [22]
	230℃ - 330℃	Thermal decomposition of the hemicelluloses and glycosidic links of cellulose	
	328.9℃	Decomposition of Cellulose I and complete decomposition of ∝-cellulose	
	481℃	Degradation of Lignin	
	500℃ above	Molecules breakdown into low molecule weight products, such as CO, CO_2, H_2O, hydrocarbons and hydrogen	

According to all above findings, it is evident that the fibre extraction methods have an effect on their properties.

CHAPTER 3: METHODOLOGY

3.1 Material collection

Different morphological varieties of LS were identified from the planters through Department of Agriculture, Sri Lanka. Three types of LS plants were identified with variations in its leaf characters. Lamina-dissected form with dissected leaves, Sagittate form with non-dissected leaves and Mixed form with both dissected and sagittate types of leaves were found in the field research. Rarely found the Mixed form of LS plants in the growing areas.

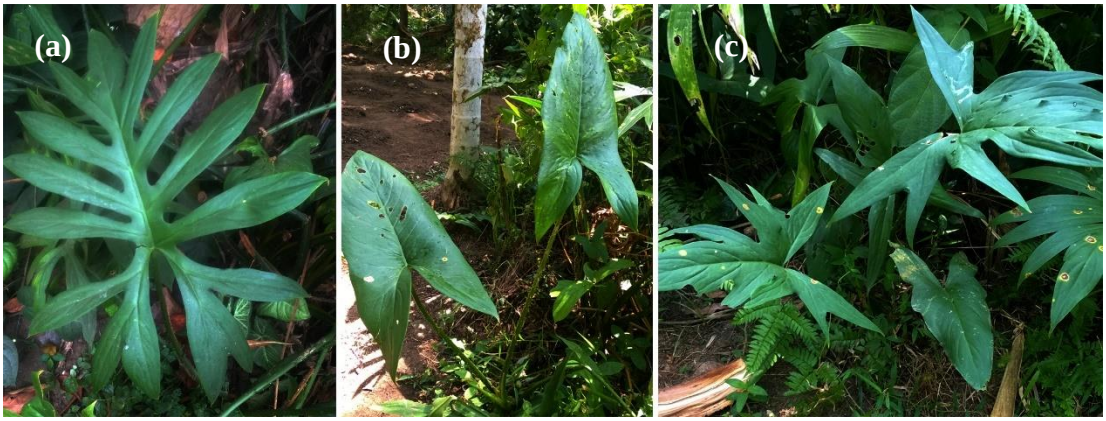

Figure 3.1: Identified LS types (a) LD type, (b) SG type, (c) Mixed type

Lamina-dissected type and Sagittate type plants were selected for the fibre investigations due to their widespread availability in Sri Lanka. Well grown rhizomes in equal age of the identified two plant types were collected from LS cultivators. Each collected rhizome, approximate 30cm long parts were cut and separated in to three pieces. Three pieces were named as tip part, middle part and the latter part according to the maturity of rhizome formation. Tip part is where the leaves are grown out from, middle part is next to the tip part and the latter part is the underground part with roots. Mud and outer core with the pointy spine of the collected rhizomes were removed and separated for fibre extraction.

Figure 3.2: LS rhizome preparation for fibre extraction (a) pointy spines, (b) Separated rhizomes into different maturity levels, (c) Pointy spine and mud removed rhizomes

3.2 Extraction procedure of fibre from rhizome

3.2.1 Mechanical extraction

In mechanical extraction, it is required to have a scoring blade or a sharp knife with a table lamp like light source. Using a sharp knife, a shallow cut was introduced around the epidermis of spines and mud removed rhizome. Then the rhizome was split along the cut and the two parts were separated and moved away from each other. This will result in the formation of fibre belonging to the two rhizome parts and further movement will enhance the formation of more fibre as shown in Figure 3.3.

Extracted fibres were viewed under a light microscope for the understanding of the structure of them.

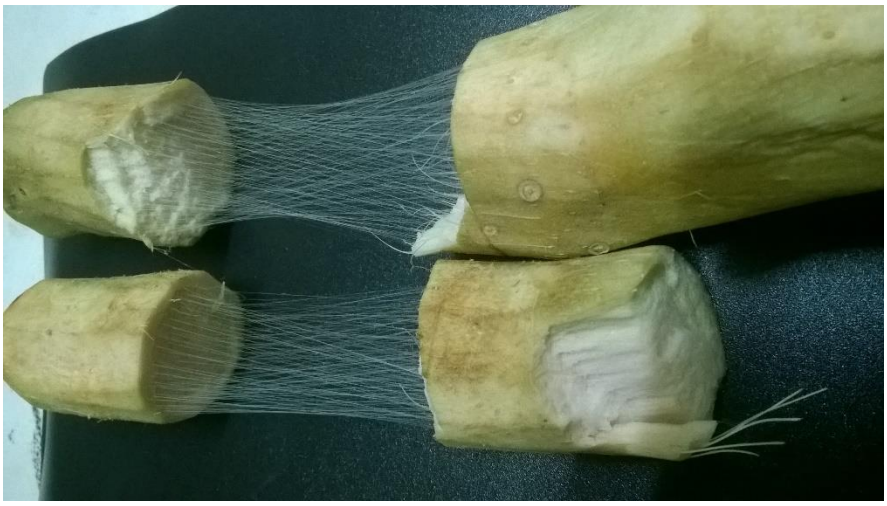

Figure 3.3: Mechanical fiber extraction from split rhizome

3.2.2 Alkali extraction

Alkali extraction method was tested in extracting fibres from LS rhizomes. Cleaned rhizomes were boiled in 5% NaOH solution for 2 hours as in the Figure 3.4. The fibres separated by removing the flesh of the rhizomes could be observed as shown in the Figure 3.5.

Figure 3.4: Alkali extraction of LS Rhizome fibre

Figure 3.5: Alkali extracted rhizome fibre

Both the mechanically extracted fibres and alkali extracted fibres were conditioned under the standard atmospheric conditions according to the ASTM D1776 Practice for Conditioning and Testing Textiles. Fibres were kept at the temperature of 21±1℃ and under 65±2% of relative humidity conditions for 8 hours. The conditioned fibres were then taken for the microscopic analysis, moisture absorbency test and for the tensile testing.

3.3 Morphological studies

The anatomy analysis of the LS rhizome was done by the Olympus BX61 motorized upright microscope and the rhizome fibre morphology was examined using light microscope and the Scanning Electron Microscopy [SEM]. ZEISS EVO 18 Research scanning electron microscope was used to observe the morphology of the fibre. In order to get high-quality detailed views of the fibre samples, fibres were sputter coated with a thin gold layer prior to them were loaded in to the SEM. Coated fibre samples were mounted on aluminium holders and placed inside the vacuum chamber of the SEM for image generation. High energy electron beam is radiated to the fibre sample and scans the surface of the sample and generate secondary electrons. These secondary electrons together formed high quality SEM images of the fibre samples. The SEM monographs were generated at the resolution range of 150 X -15 KX.

Freeze fracture method was applied on mechanically extracted fibres using liquid nitrogen to investigate the cross section of LS fibre. Mechanically extracted fibres from a LS rhizome was placed on top of a porcelain source and poured liquid nitrogen on to fibre and fractured it. Fractured fibre was taken to the SEM and observed the cross-sectional views of the LS fibre. Same test was performed on fibres extracted from the rhizomes of both the types of LS plants.

3.4 Fourier Transform Infrared Spectroscopy [FTIR]

Bruker Alpha II Fourier Transform Infrared [FTIR] Spectrometer was used to obtain the FTIR spectrum of LS fibre in KBr matrix with 28 scans at a resolution of 4 cm^{-1}between the wave number region of 600 – 4000cm^{-1}. The mechanically extracted and the NaOH extracted fibres were oven dried at 105 ℃ for 2-4 hours and grounded into fine powder using mortar and pestle. Then the powdered fibre was grounded with IR transparent potassium bromide (KBr) and pelleted to generate spectrum under standard conditions. Both the mechanically extracted and alkali extracted fibres from lamina dissected type and the sagittate type plants were investigated and the FTIR spectrums obtained were used to determine the chemical groups presented in fibres.

3.5 X-Ray Diffractometer analysis

Powdered samples of LS plant fibres were subjected to X-Ray diffraction in Bruker D8 Discover X-Ray Diffractometer to investigate the crystallinity index and crystal size. Electromagnetic radiation is used in the X-Ray diffractometer to substantially produce a diffraction pattern on a screen.

3.6 Moisture regain

Fibre samples were tested following the ASTM D2495 -07 Test Method for Moisture in Cotton by Oven-Drying. Mechanically extracted fibres were prepared for the moisture regain test as follows.

- Mechanically extracted fibres from lamina dissected type and the sagittate type LS plants were conditioned under 65% relative humidity and 21℃ for 8 hours.

• Sufficient number of empty weighing bottles were also kept under the same conditions and measured the weight of the individual bottles and 5g of fibre samples from each plant type was measured and taken for oven drying in weighing bottles.

• Conditioned fibre sample each weight of 5.000g to 6.000g was added in to the weighing bottles and measured the fibre weight in weighing bottles.

• Weighing bottles with the fibre samples were then oven dried at 105 ± 2 ℃ (220 ± 4 °F) until the change in mass between two successive weighing at intervals of 1 hour is less than 0.1% of the sample mass. Weighing bottles open and lids of the bottles were kept separately inside the oven.

• When reaching one-hour intervals, weighing bottles with fibre were tightly closed with their lids and taken out from the oven and stored in to the desiccator. Desiccator was used to cool the specimen and the weighing bottles to the room temperature and to transport fibre with the container to the electric balance for weighing and to return back to the oven at successive weightings.

• Repeat the drying, cooling and weighing at 1-hour intervals until the change in mass between two successive weighing at intervals of 1 hour is less than 0.1% of the sample mass.

• Final mass of the container with oven dried fibre samples were recorded.

• Five fibre samples from each plant type was tested and the mean value of the moisture content and moisture regain was calculated.

3.7 Tensile test

The single fibre tensile strength was determined using the universal tensile testing machine, INSTRON 4466 following the ASTM D3822-14 standard. 10mm/min cross head speed and 50 mm guage length were employed and tested 30 number of both Lamina dissected type fibres [LDTF] and Sagittate type fibres [SGF]. Linear density of the fibres was determined in accordance to the ASTM D1577-07 standard. Fibre specimens were prepared for the testing's as follows.

3.7.1 Fibre linear density

• Fibre testing was performed at the standard atmospheric conditions of 65±2% relative humidity and 21±1℃ temperature.

• Mechanically extracted LDTF and SGF were cut into 90mm length using a sharp blade.

• Weight of the two types of specimens were measured separately.

• Number of fibres in each fibre bundle were counted and recorded.

• Using the obtained measurements, the tex count of the LS fibre was calculated

3.7.2 Fibre tensile behavior

• Mechanically extracted fibres from lamina dissected type and the sagittate type LS plants were conditioned under 65% relative humidity and 21℃ for 8 hours.

• The smallest visible fibre to the naked eye from the rhizomes of each plant type were extracted mechanically and mounted on square shaped paper frames of 60mm x 60mm making the gauge length of fibre for the testing as 50mm. 30 paper frames with pasted fibres were prepared from the fibres of each plant type. As the fibre consist with crimp, it was subjected to pretension according to the standard.

• The distance between the clamps of the INSTRON machine was adjusted to 50 mm with 50 kN load cell and prepared the machine for the testing.

• Each specimen was tested and recorded the force applied at the breaking point in N and the fibre extension in mm as displayed in the machine.

• Each fibre breaking tenacity was calculated with the use of breaking force and the linear density of the respective plant type of the LS plant.

• Fibre elongation and the Young's modulus was calculated for each fibre.

• Mean value and the standard deviation of the tenacity, elongation and the Young;s modulus was calculated using following equations.

Equation 1

$$\text{Tensile Strength} = \frac{F_{\text{at breat}}}{\text{Linear Density (tex)}}$$

Equation 2

$$\text{Breaking Elongation} = \frac{\Delta L}{L} \times 100$$

Equation 3

$$\text{Young's Modulus} = \frac{\frac{F_{\text{at break}}}{\text{Linear Density (tex)}}}{\frac{\Delta L}{L}}$$

3.8 Dye up-take behavior

Dye absorbency behavior of LS fibre was investigated applying scouring, bleaching and dyeing processors for a woven textile sample from its rhizome fibre.

3.8.1 Preparation of yarns and fabric

- Mechanically extracted fibres from both LDTF and SGF were subjected to yarn preparation by hand twisting on a wetted surface.
- Continuous strand of yarn was prepared and wounded on to a thin wooden strip.
- Warp prepared on a 5" x 8" frame loom with the wounded yarn to the wooden strip.
- Inserted the weft yarn and prepared a woven textile sample on the frame loom.
- Sample preparation was carried out under standard atmospheric conditions of 65±2% relative humidity and 21±1℃ temperature.
- Conditioned textile sample weight was measured and recorded.

Figure 3.6: LS woven textile sample

3.8.2 Scouring

Scouring was performed to remove the impurities contaminated on fibres to improve the dye absorbency. Table 3.1 shows the recipe followed in scouring.

- Measures of each ingredient were calculated according to the weight of the LS textile sample.
- Raw cotton textile sample in the same weight was also taken for the scouring to compare the dye absorbency results of the LS fibre versus cotton fibre at the end of the testing.

Textile sample weight = 3.5g

Table 3.1: Scouring recipe

Ingredients	**LS textile**	**Cotton textile**
Distilled water (ml) 1:50 ratio	175	175
Wetting Agent (g) 10:1 ratio	0.35	0.35
NaOH (g) 1:1 ratio	3.5	3.5

- Both the LS and raw cotton textile samples were kept in the above solution for 20 minutes at 95℃ on a hot plate.
- Scoured textile samples were hot washed and taken for bleaching.

3.8.3 Bleaching

Both the scoured textile samples were bleached with recipe in table 3.2 for further removal of natural coloring matters on fibres.

- Measures of each ingredient were calculated according to initial weight of both the LS and cotton textile samples.
- Both the samples were kept in the solution for 20 minutes at 80℃ on a hot plate.
- Bleached textile samples were hot washed and dried.

Table 3.2: Bleaching recipe

Ingredients	LS textile	Cotton textile
Distilled water (ml) 1:50 ratio	175	175
Wetting Agent (g) 10:1 ratio	0.35	0.35
NaOH (g) 1:1 ratio	3.5	3.5
Sodium silicate (g) 3:1 ratio	1.16	1.16
Hydrogen peroxide (ml)	2.85	2.85

• Weight of the dried samples were measured and recorded.

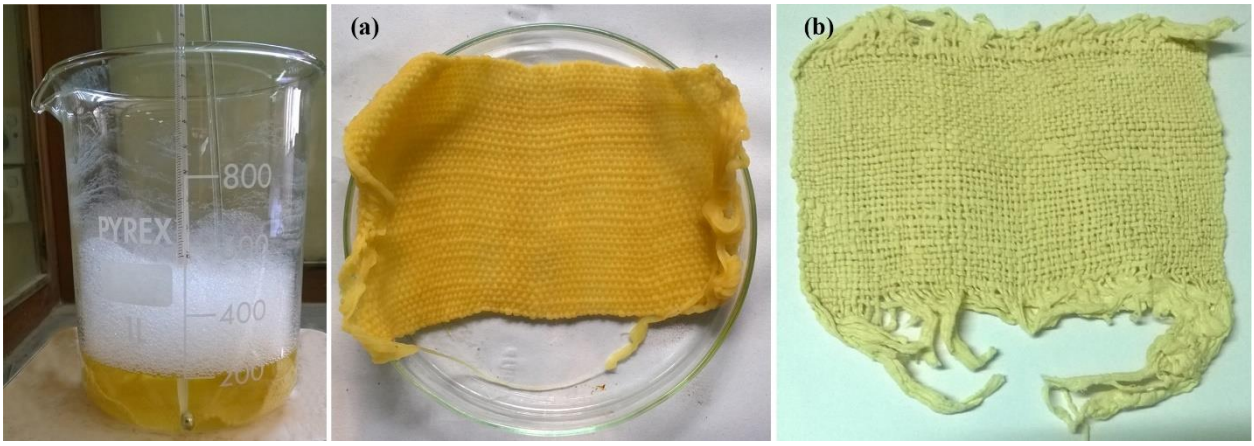

Figure 3.7: Bleached LS textile sample (a) wet condition (b) dry condition

3.8.4 Dyeing procedure

Most commonly reactive dyes are used to dye cellulose materials. Hence, it was decided to use reactive dyes to dye both the textile samples.

• Bleached textile samples were oven dried to remove the moisture and measured the weight of each samples.

• Measures of the distilled water and chemicals needed for sample dyeing were decided according to the weight of the oven dried LS textile sample. Following recipe was followed in dyeing the samples under different conditions.

Table 3.3: Dye recipe

Ingredients	**LS textile** **Oven dry Weight = 1.741g**	**Cotton textile** **Oven dry Weight = 1.741g**
Reactive dye (g) (2% from the sample weight)	0.07g	0.07g
Distilled water (ml) total solution (Ratio for sample weight 1:50)	87.05ml	87.05ml
NaCl (g) (50g per 1000ml)	4.4 g	4.4g
$NaCO_3$ (g) (20g per 1000ml)	0.16g	0.16g
Soaping (g/l) (5g per 1000ml)	1.25	1.25

• Both LS and cotton textile samples were kept in the dye solution under 50℃ for 15min.

• Half of the measured NaCl was mixed with the dye solution and kept under 50℃ for 15min.

• Balance NaCl amount was mixed with the dye solution and kept under 50℃ for another 15min.

• $NaCO_3$ was added and the whole solution was kept under 50℃ for another 45min.

• Dyed samples were washed in cold water for 10 min and rinsed with non-ionic detergent at 60℃ for another 10 min and kept for drying.

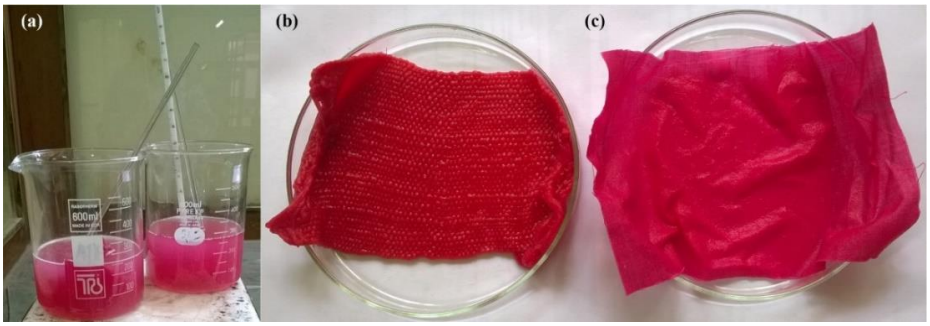

Figure 3.8: Dyed LS textile samples in wet condition (a) Dye solution with samples, (b) Dyed LS sample in wet condition, (c) Dyed Cotton sample in wet condition

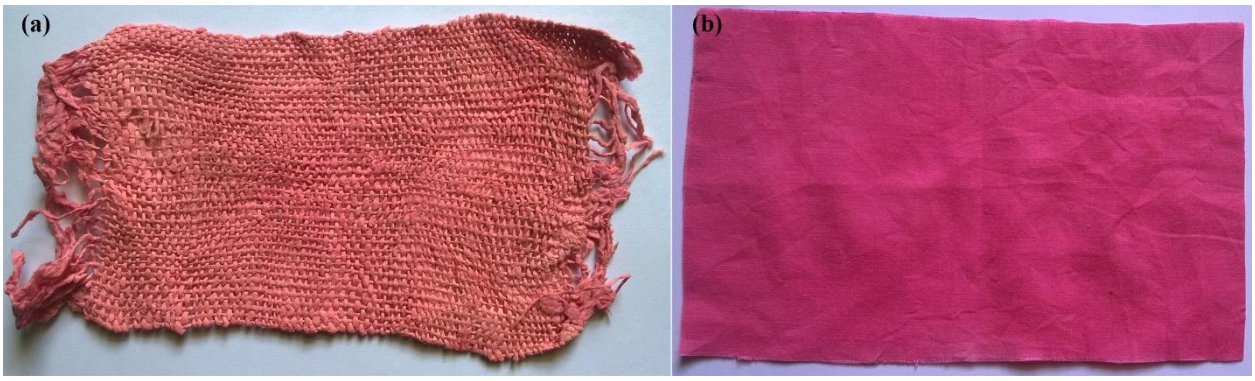

Figure 3.9: Dyed textile samples in dry condition (a) Dried after dyeing - LS samples, (b) Dried after dyeing - Cotton samples

• Colour measurements, whiteness index was taken from the Datacolor 800 Spectrophotometer.

• Whiteness of the textile samples were compared.

3.9 Thermogravimetric analysis (TGA)

Thermal stability is an important characteristic to investigate in fibre characterization to decide the application of the fibre for high temperature applied manufacturing processes. Thermogravimetric analysis of both the LDTF and SGF was carried out in SDTQ600 Thermo Gravimetric Analyzer. The spectrum was recorded within the temperature range of ambient to 800℃ under high purity nitrogen gas atmosphere at a heating rate of 10℃/min.

CHAPTER 4: RESULTS AND DISCUSSION

4.1 Rhizome anatomy

LS plant belongs to the Araceae family [10] and included under monocotyledonous flowering plants [13]. Monocot rhizome anatomy consists with the features such as randomly placed vascular bundles and absences of secondary walls.

Well grown LS rhizome cross section was studied to obtain an understanding of its anatomical structure through optical microscope. Figure 4.1 presents the naked eye view of the rhizome cross section and longitudinal section while Figure 4.2 represents the micrograph of a transverse section of the rhizome cross section.

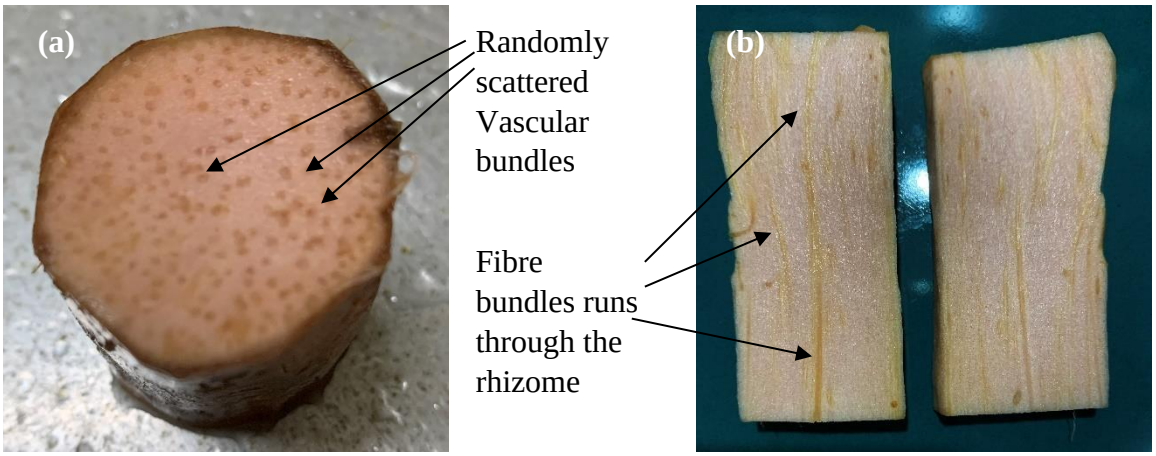

Figure 4.1: Naked eye view of rhizome (a) cross section, (b) longitudinal section

Vascular bundles placements are clearly visible on the rhizome cross section (dark colour spots). Nearly 100- 120 possible sites for the formation of vascular bundles appeared on this cross section and further it was seen that a higher number of vascular bundles were formed when extracting was done. The longitudinal sections of LS rhizome in Figure 4.1 (b) shows the formation of the fibre bundles along the rhizome. As in Figure 4.2 it is observed that the rhizomes are consisted with two types of fibres. (a) Thick fibre strands that are shorter in length and (b) thin long fibres. At further investigation, it is identified that the composition of two fibre types in a rhizome are varied according to the maturity level of it. Thick fibre strands were absent in immature rhizomes. However, there were

few fibre strands evident at the middle part and higher number in matured end part of the rhizome.

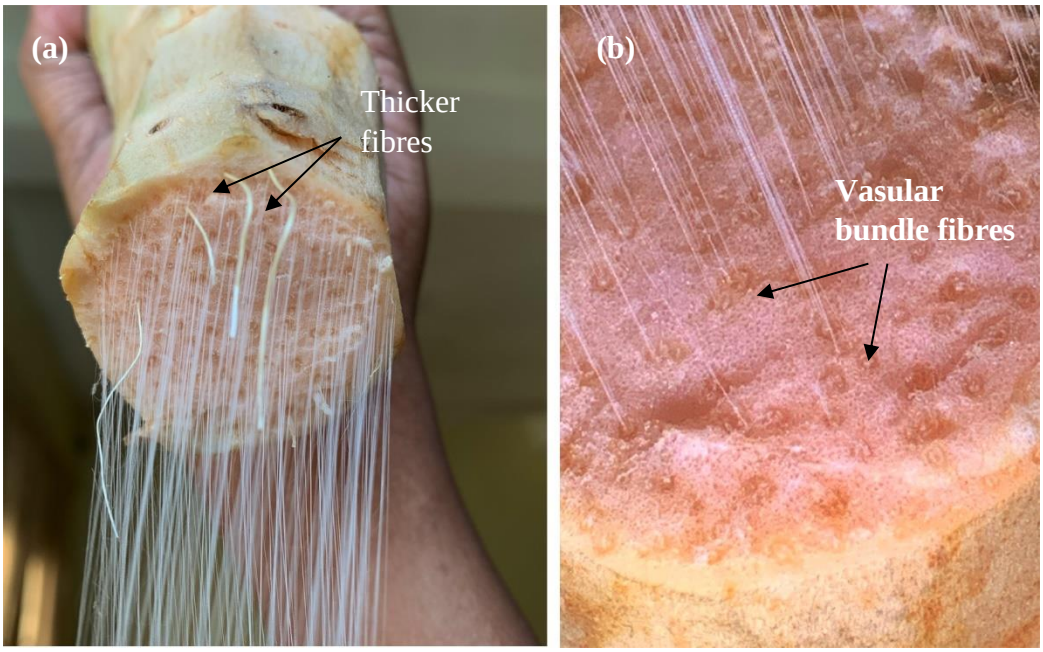

Figure 4.2: LS Fibre types (a) thick and thin fibres, (b) vascular bundle fibres

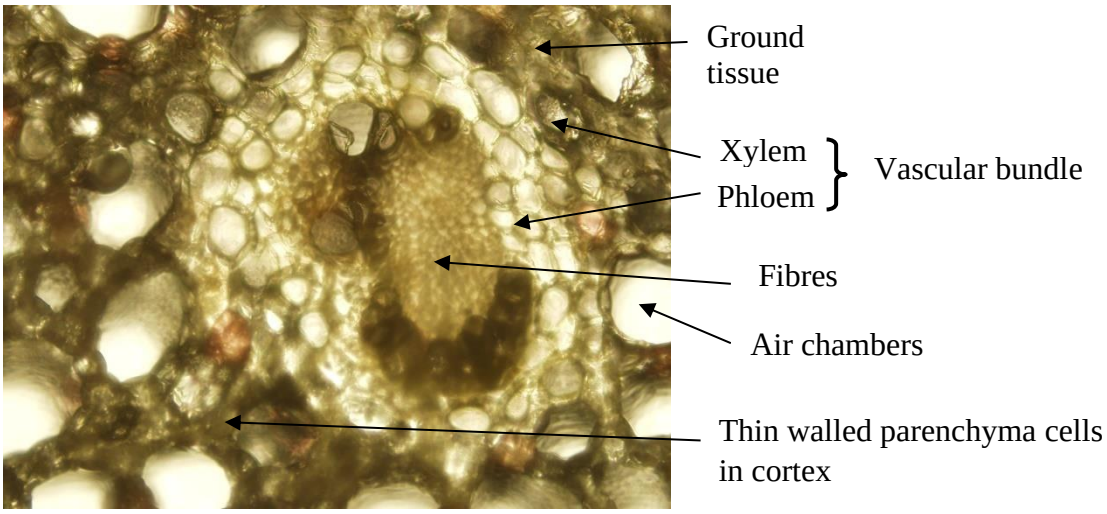

Figure 4.3: Micrograph of the transverse section of LDT rhizome at 5 X 10

Randomly scattered vascular bundles are appearing in the ground tissue of the rhizomes. Fibre bundles are surrounded by phloem and xylem cells. Further it was observed that the secondary growth is absent due to an absence of cambium of monocotyledonous type plat

rhizomes. The thin walled parenchyma cells and air chambers are clearly visible in the Figure 4.4.

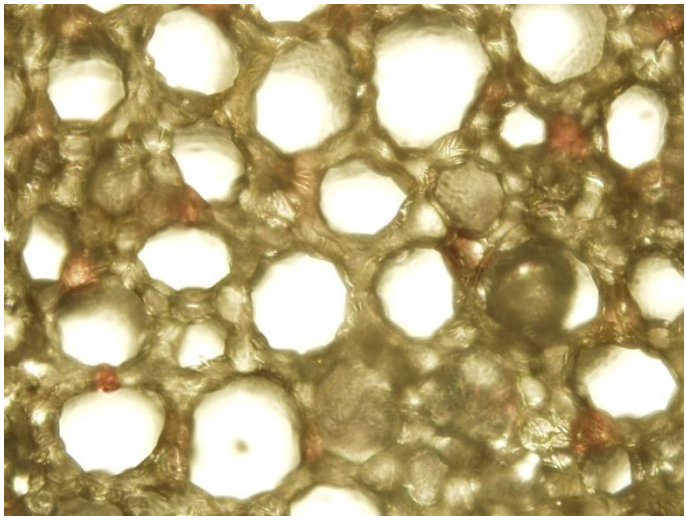

Figure 4.4: Thin walled parenchyma cells and air chambers at 5 X 10

Transverse sectional micrograph of the Sagittate plant rhizome shows the same cell arrangement as presented in the Figure 4.5.

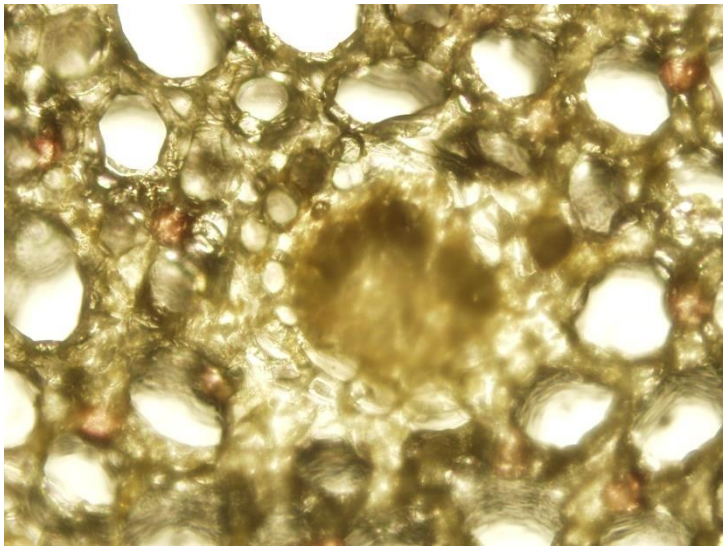

Figure 4.5: Micrograph of the transverse section of SG at 5 X 10

4.2 SEM analysis of the *Lasia spinosa* fibre

The light microscope image of a Lamina dissected type LS rhizome fibre is shown in Figure 4.6.

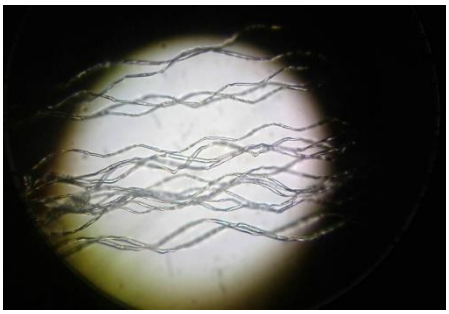

Figure 4.6: Light microscope image of a LS rhizome fibre 4X 10

The SEM morphology of the mechanically extracted and the alkali extracted rhizome fibre of LDT type and the SG type are shown in the Figures 4.7,4.8,4.9 & in 4.10.

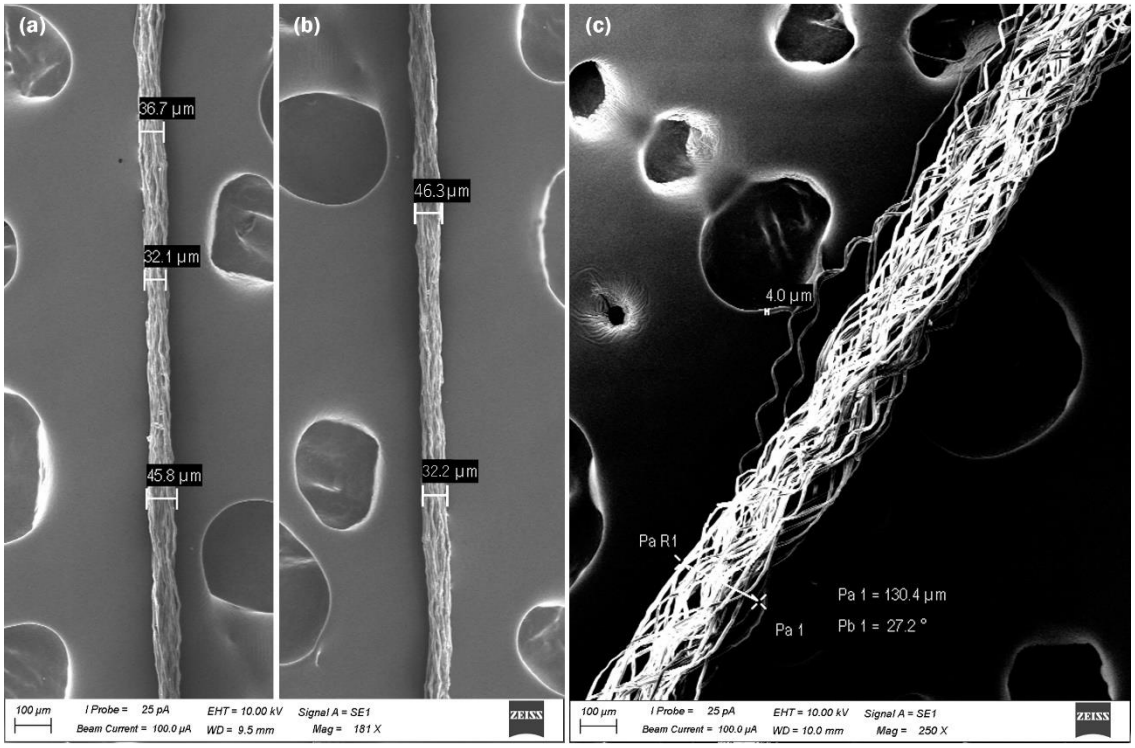

Figure 4.7: SEM images of LS Fibre (a) LDTF, (b) SG, (c) formation of fibrils

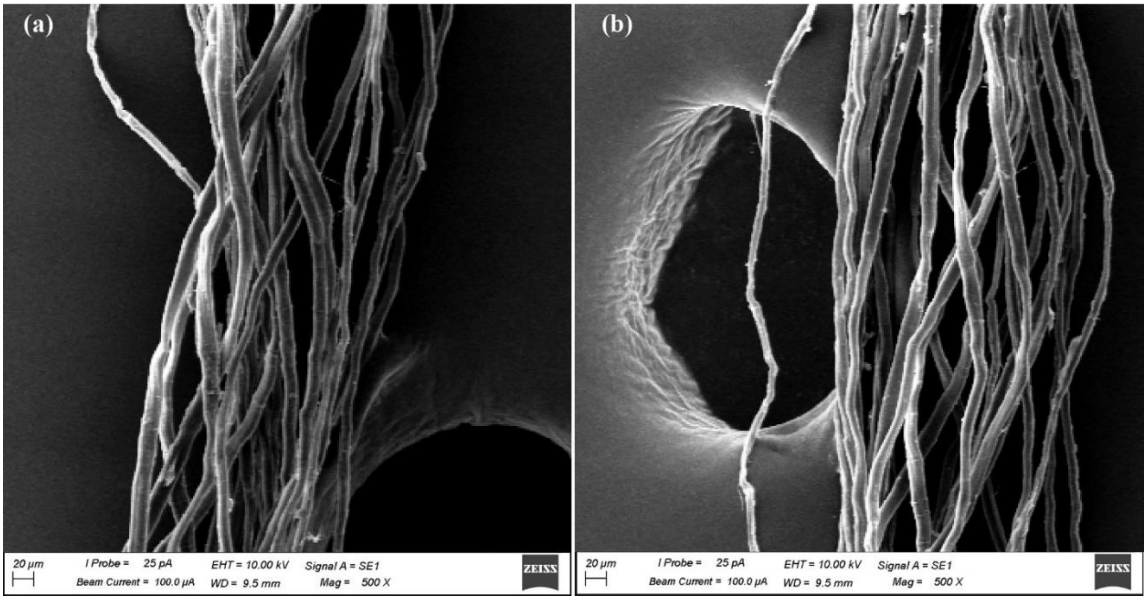

Figure 4.8: SEM images of raw rhizome fibre fibrils (a) SGF (b) LDTF

SEM images in the Figures 4.7 and 4.8 reveal that the rhizome fibres of both LS plants have very similar morphology and have cylindrical shaped fibrils which are oriented along the fibre axis in a loose manner. Fibre diameter is varied along the length of the fibre due to the uneven formations of fibrils. As per the SEM images of the fibre, it is clearly evident that the diameters of the fibres are vary in between the range of 31 µm – 47 µm. However, this variation may depend on the maturity level and the growing conditions of the plants. According to the Figure 4.7 (c), fibrils have an inherent crimp and organized in a helical manner. As per the image in the Figures 4.8 (a) and (b), the number of fibrils in a fibre lies in the range of 16-25. According to the Figure 4.9 and 4.10, it is evident that the diameters of the fibrils are different to each other and lies in the range of 2.5 µm – 6.5 µm. Unlike the literature [6], [8], [9], the LS rhizome fibres does not have any microfibrils. SEM micrographs indicate that the fibril surfaces have a rough appearance with randomly deposited impurities on the surface.

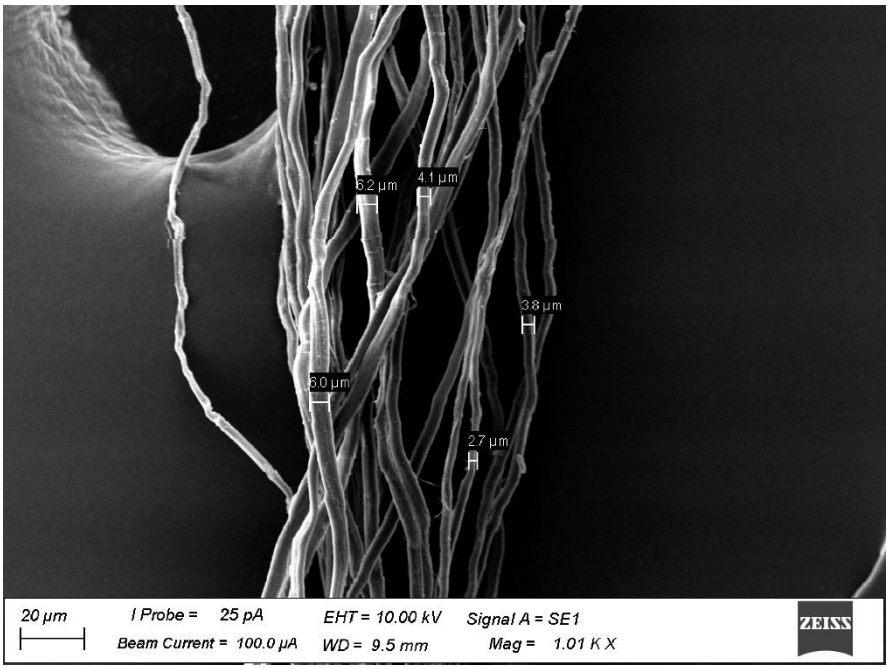

Figure 4.9: Range of diameters in fibrils of LDTF at1.01 K X

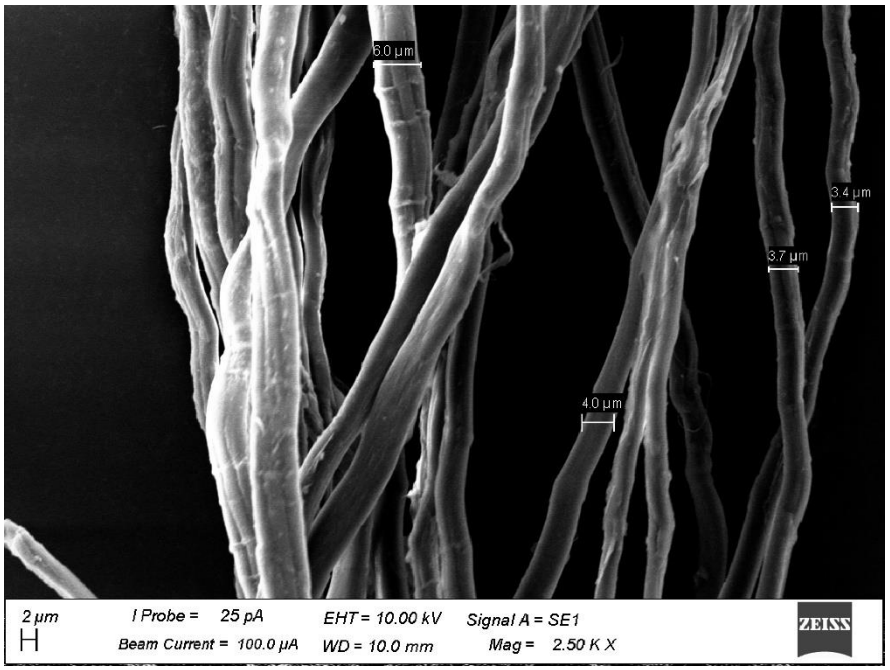

Figure 4.10: Range of diameters in fibrils of LDTF at 2.5 K X

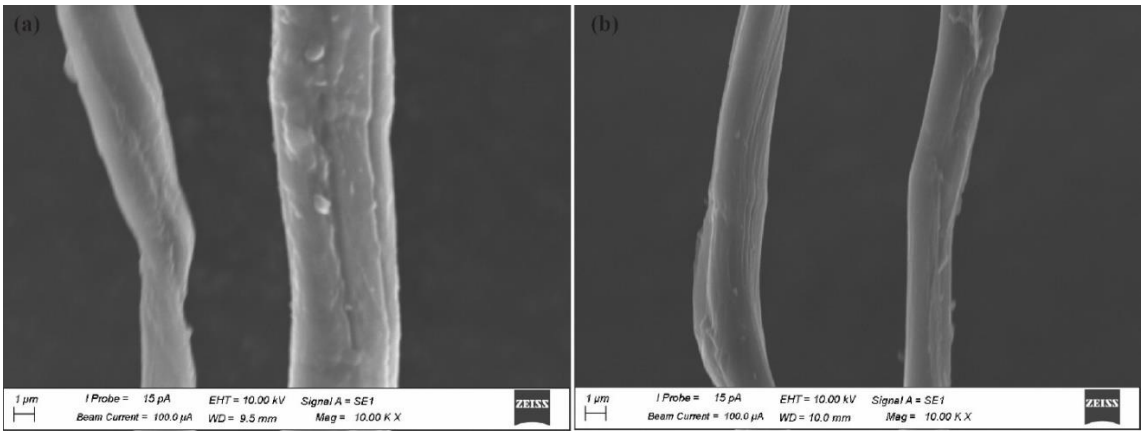

Figure 4.11: Raw and Alkali extracted LDTF fibre (a) Raw LDTF fibrils, (b) Alkali treated LDTF fibrils

Samples of mechanically extracted and alkali treated fibres were viewed through the SEM in order to understand any changes to the surface appearance caused by NaOH treatment. Images in the Figure 4.11 reveal that the hand extracted fibril surface contains impurities on it. Rough and uneven textural look appears on the surface of the mechanically extracted fibre fibrils as stated by Indran et al. [22] and Senthamaraikannan [38] due to cavities with small voids, contaminated pectin, lignin, oil and impurities. Such impurities are not evident on alkali extracted fibres. NaOH extracted fibre fibril surface shows the removal of contaminants on the surface of them and result with a clear and smoother surface with the absence of larger contaminants, but with very fewer solid aggregates were seen which is an improvement in comparison with the mechanical extraction method. As investigated by several researches, such as Senthamarikannan [38] and Cheng [40], alkali treated fibril surfaces are evident with the absence of pectin, lignin, oil and impurities while improving their surface properties. The same result is retrieved by the SEM images of the mechanically extracted and NaOH treated LS fibre as in Figure 4.11.

Freeze cut fibres by the liquid nitrogen revealed a clear morphology of the cross section of a fibril as in Figure 4.12. It is evident that the fibril has a primary wall and several other secondary walls formed towards the middle of the fibril. A string of cellulose crystals linked along the fibril axis by disordered amorphous domains in the LS fibre were evident as shown by Carrasco [31] in the investigation of wood fibre.

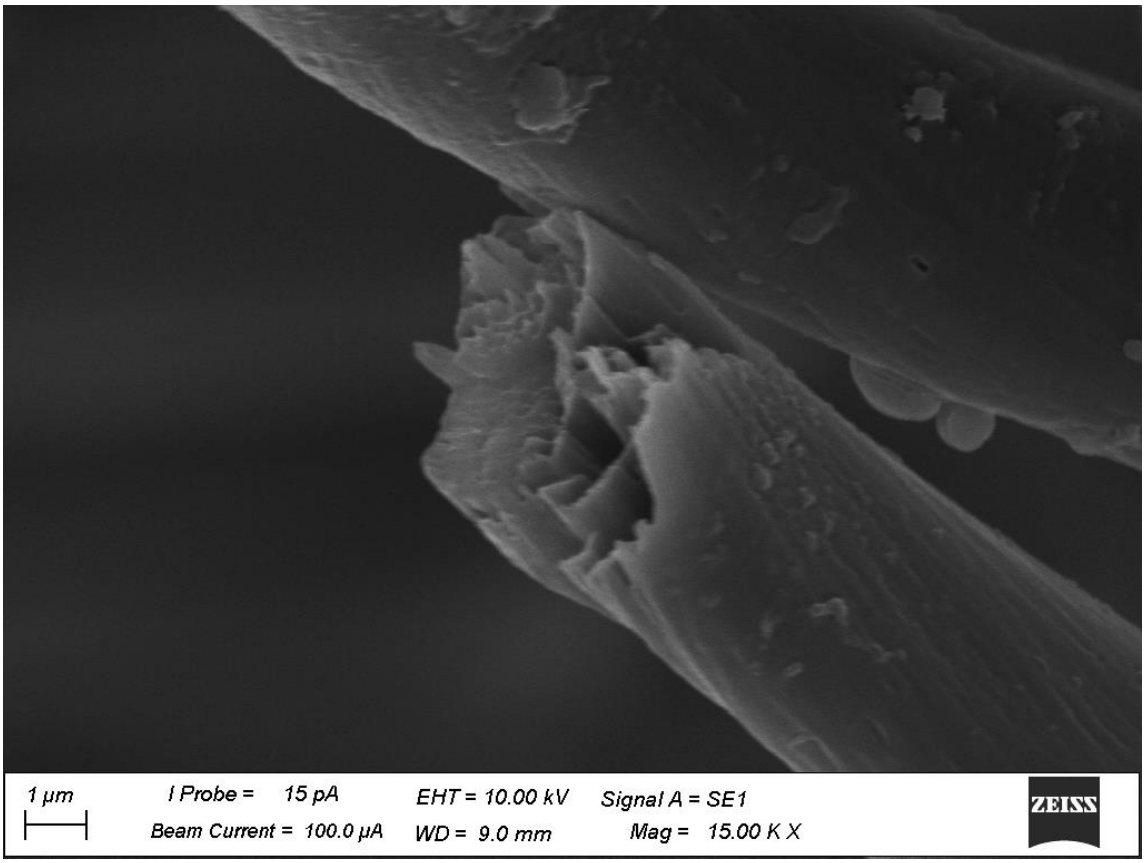

Figure 4.12: Cross section of fibril at 15K X

It is observed that the fibres form spirals with a natural crimp. Mechanically extracted fibres have a good stretch ability and it is confirmed by these SEM images of crimpy microfibrils. Figure 4.13, 4.14 and 4.15 show the crimp in microfibrils at different magnifications. With these observations, it can be concluded that the LS fibre is a crimpy fibre. During the mechanical extraction of fibre, it was observed that the original length measured at the point of extraction was reduced after a few minutes due to the possible relaxation of the crimp.

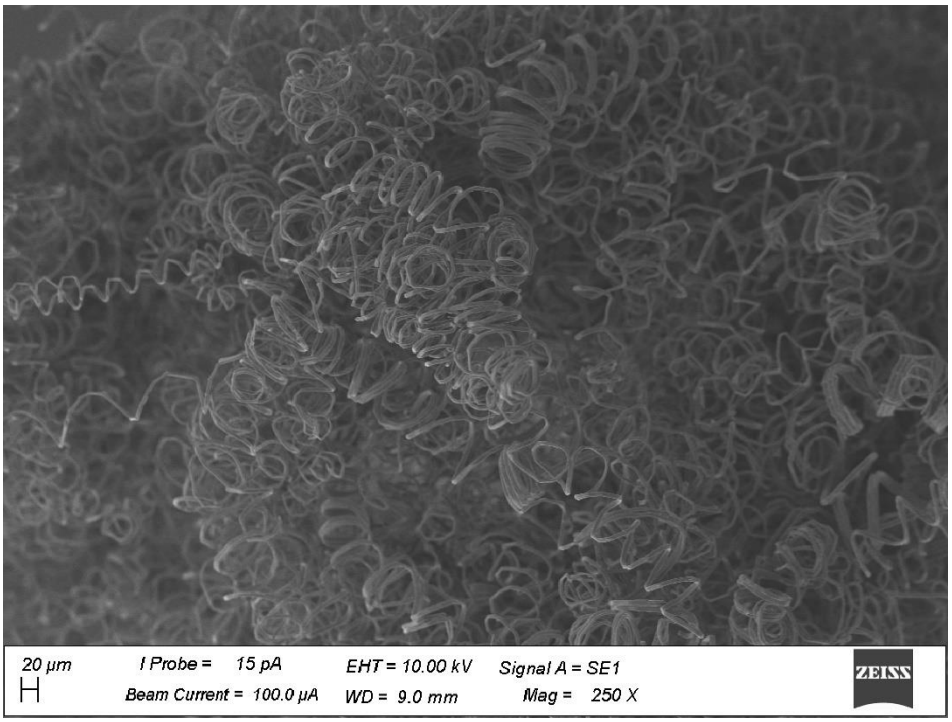

Figure 4.13: Crimp in LS fibrils at 250 X

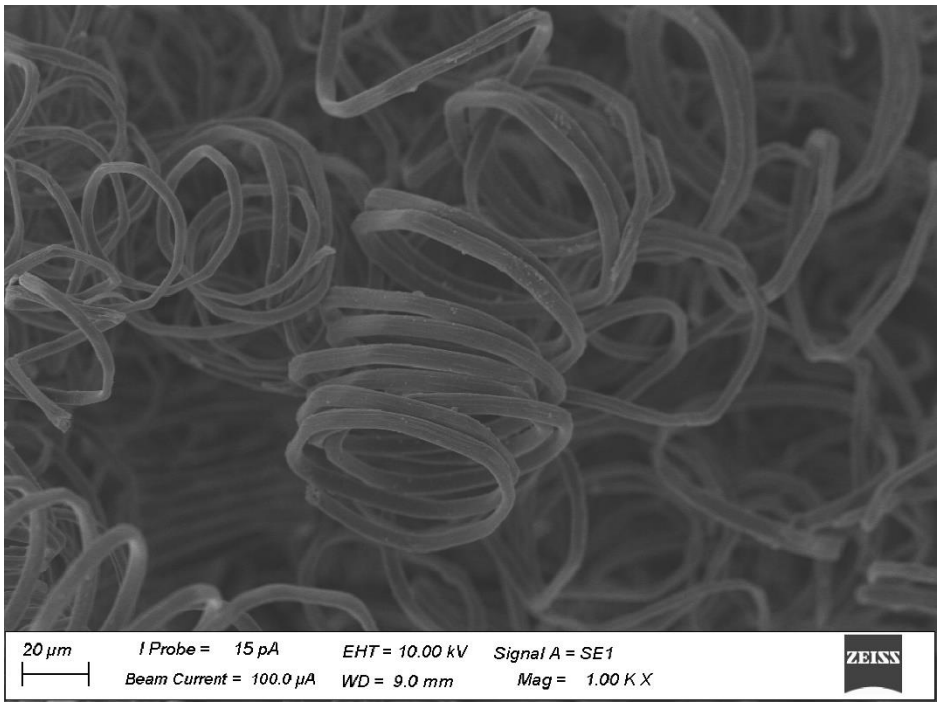

Figure 4.14: Crimp in LS fibre at 1.0 K X

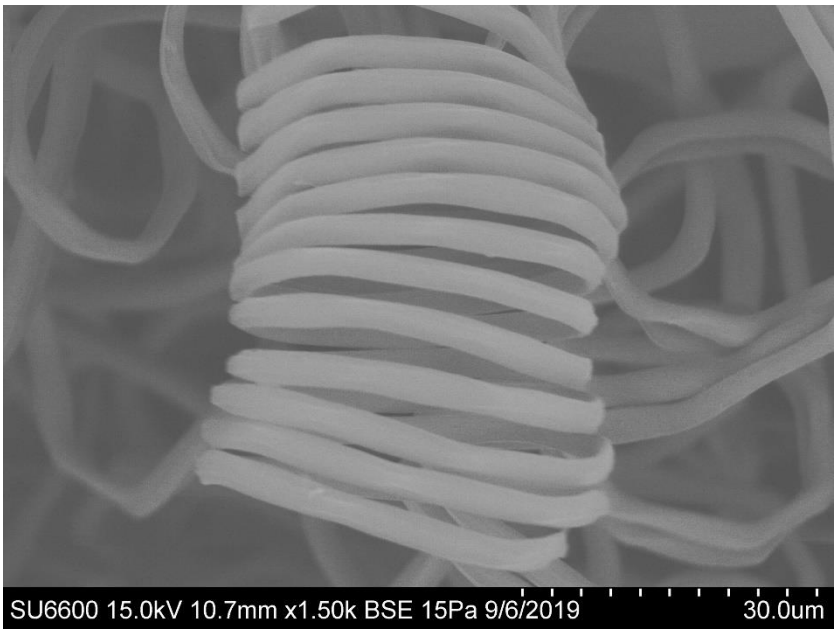

Figure 4.15: Crimp in LS fibre at 1.5 K X

Further it is observed that the fibrils are interconnected at certain places with other fribrils by natural compounds in its formation. Figure 4.16 shows fibril bonds of LDTF and SGF.

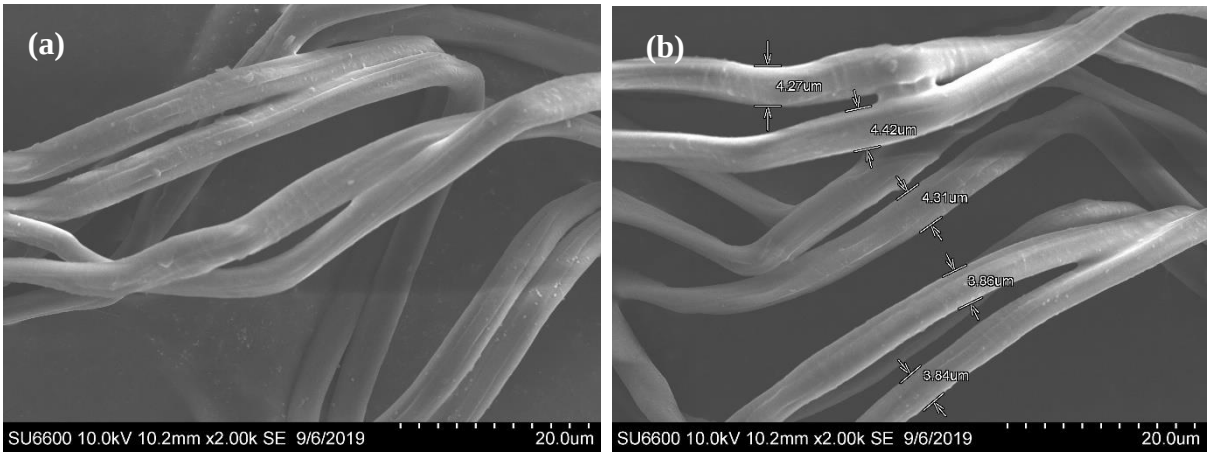

Figure 4.16: Fibril bonds (a) LDTF and (b) SGF

In addition to the above fine fibres, there are thick shorter fibres formed in LS rhizomes. These types of fibres are mostly appear in maturing rhizomes. Micrographs of mechanically extracted thicker fibres are shown in the Figures 4.17 and 4.18. Diameter of

thicker fibres ranges from 318 µm to 350 µm. Higher number of cavities with voids and contamination with natural compounds appear the surface of the fibre.

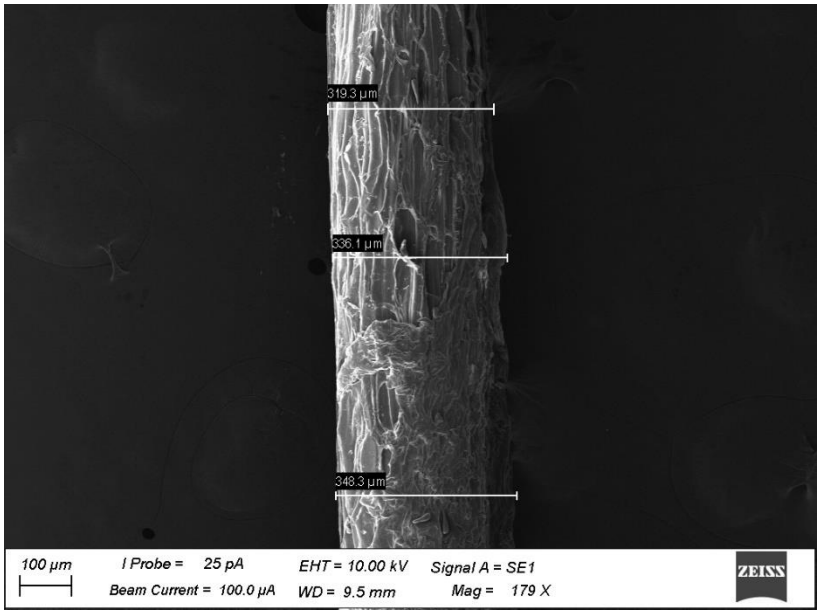

Figure 4.17: SEM micrograph of thicker fibres at 179 X

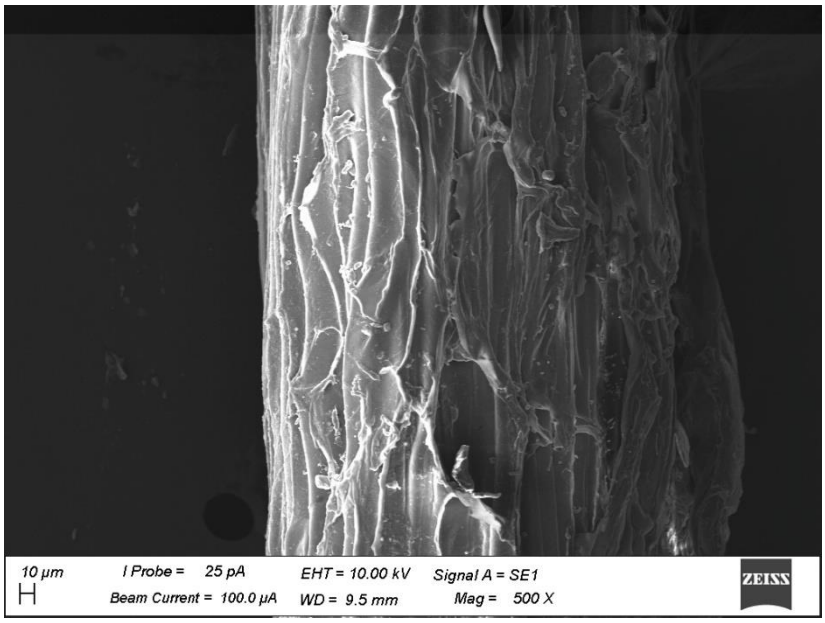

Figure 4.18: SEM micrograph of thicker fibres at 500 X

As observed in this investigation, the density of the thick fibres in rhizomes increases with the rise of its maturity level. This is possible due to the starch deposition and lignification process of plant cells that increase with the age of the plants as stated by Wahab [43] in the investigation of Bamboo fibre.

4.3 FTIR analysis

The FTIR spectrums of LDTF and SGF are shown in the Figures 4.19 and 4.20. Those spectrums give a qualitative indication about the chemical structure of the LS rhizome fibre. Spectrums present the IR transmission values within the wave range of 500 cm^{-1}-4000 cm^{-1}. Though the shapes of the spectra obtained from both LS plant types appear basically similar to each other, the transmittance values were slightly different. IR absorption bands in the FTIR spectrums of fibres, indicate the vibration modes such as stretching, bending or wagging of chemical bonds present. The obtained FTIR spectrums were compared with the findings in literature review.

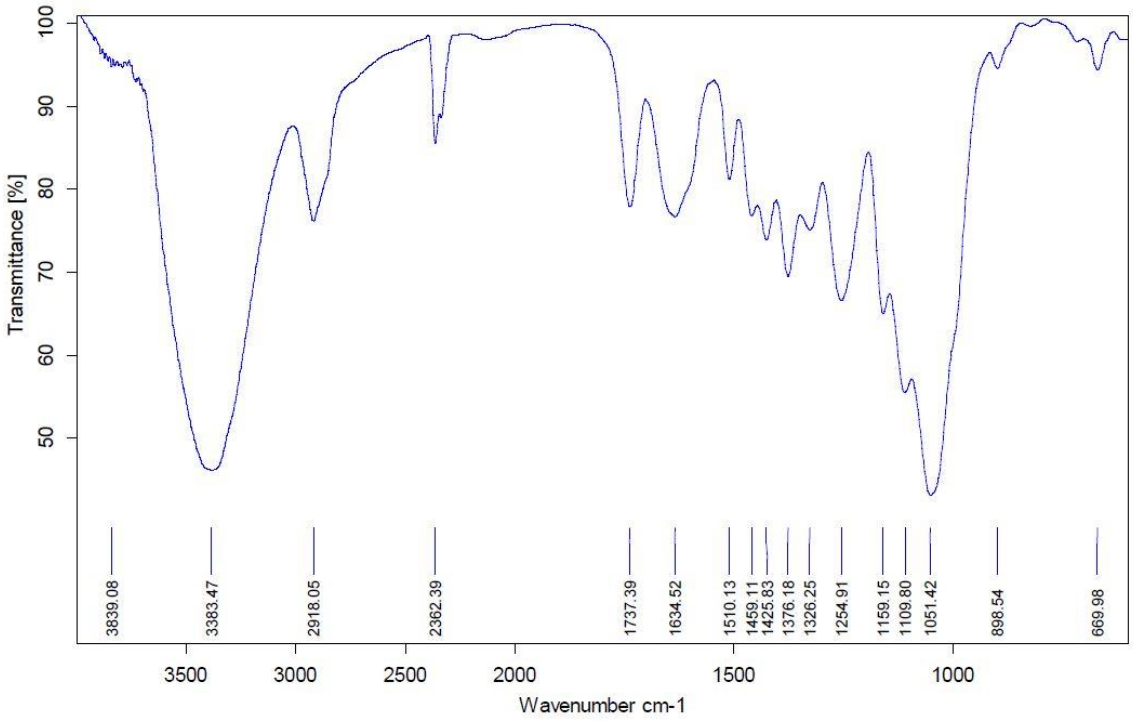

Figure 4.19: FTIR Spectrum of LDTF fibre

Sharp peaks are evident at the wave numbers of 3383 cm^{-1}, 2918 cm^{-1},2362 cm^{-1}, 1737 cm^{-1}, 1634 cm^{-1}, 1510 cm^{-1}, 1425 cm^{-1}, 1376 cm^{-1}, 1254 cm^{-1}, 1159 cm^{-1} and 1051 cm^{-1}.

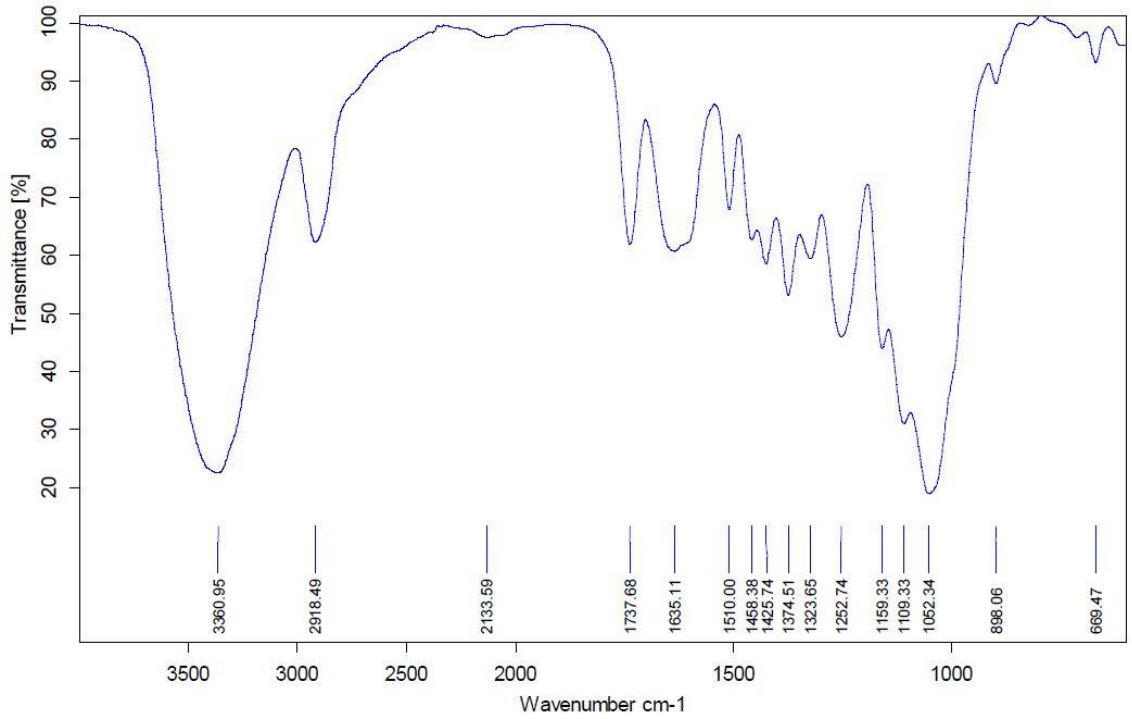

Figure 4.20: FTIR Spectrum of SGF fibre

According to the SGF, it shows clear bands at the wave numbers of 3360 cm^{-1}, 2918 cm^{-1}, 1737 cm^{-1}, 1635 cm^{-1}, 1510 cm^{-1}, 1425 cm^{-1}, 1374 cm^{-1}, 1252 cm^{-1}, 1159 cm^{-1} and 1052 cm^{-1}. When the wavenumbers indicated in Figure 4.19 and 4.20 are compared, it can be concluded that the chemical groups presented in both plant type rhizome fibres are same but with slight differences in transmittance values at certain wavenumbers due to different bond vibrations connected to the placement of their groups in 3D space.

FTIR results that are obtained by different researches in their investigations on various plant fibres [18], [22], [26], [31], [35], [38] that are mentioned in the table 2.1 were taken as references to interpret the chemical groups that are presented in LS rhizome fibre. Peak position at the wave number of 3378 cm^{-1} [26], 3333 cm^{-1} [22], 3336 cm^{-1}[38], 3310 cm^{-1}[31] and 3340 cm^{-1}[35] are recorded due to the stretching of O-H bonds presence in alpha cellulose, which stand as the major component of plant fibres. Therefore, the peaks

obtained at 3383 cm^{-1}in LDTF and 3360 cm^{-1}in SGF can be considered as a result of the O-H stretching of the alpha cellulose.

Previous researchers attributed C-H stretching to peaks occurring at 2915 cm^{-1}[26], of 2800 cm^{-1} - 3000 cm^{-1} [18], 2919 cm^{-1}[22], 2919cm^{-1}[38], 2854 cm^{-1} - 2921 cm^{-1}[31] and 2915 cm^{-1} [35]. Therefore, with reference to Figure 4.19 and 4.20, it can be concluded the peaks at 2918 cm^{-1} is as a result of the stretching of C-H bonds due to the presence of alpha cellulose in LS fibres.

Several other wave numbers belong to different transmittance values are considered in identifying the chemical groups presence in LS fibre. Therefore, the peak at 2362 cm^{-1} which was presented only in LDTF could be attributed to the presence of waxes [26], [38].

Stretching of C = O groups as a result of the presence of hemicellulose in both the types of LS fibres could confirmed due to the peak at wavenumber 1737 cm^{-1} [26], [38], [20].

The peak observed at 1634 cm^{-1} in LDTF and 1635 cm^{-1} in SGF are attributed to the presence of lignin in LS fibre [38], [35].

Researchers attributed C = C stretching as a result of the presence of lignin, to peaks occurring at 1519 cm^{-1}[31], 1512 cm^{-1}[31]. Therefore, with reference to both the FTIR graphs, it can be concluded the peaks at wavenumber of 1510 cm^{-1} due to the presence of lignin in both the LS fibres.

The peak observed at 1425 cm^{-1} in both the spectrums of LDTF and SGF are attributed to the CH_2 symmetric bending of cellulose in LS fibres [22], [31], [35], [38].

The peak observed at 1376 cm^{-1} in LDTF and 1374 cm^{-1} in SGF are attributed to the C-H stretching of cellulose in LS fibre [35].

According to Maache [31], the peak positioned at the 1248 cm^{-1} is due to the C-O stretching vibration of acetyl group in lignin. Therefore presence of lignin in LS fibres is confirmed by the peaks recorded at 1254 cm^{-1} and 1252 cm^{-1} in the spectrums of LDTF and SGF respectively.

According to Belouadah [45], the peak at 1158 cm^{-1} wave number is due to the C-O-C groups of cellulose and hemicelluloses in plant fibres. Hence the peak recorded at 1159 cm^{-1} in both the LS fibres confirm the stretching of C-O-C groups of cellulose and hemicelluloses. According to Maache [31], the two peaks at 1051 cm^{-1} in LDTF and 1052 cm^{-1} in SGF are attributed to stretching of C-O bonds of hydroxyl and ether groups in cellulose.

Summary of analysis of the chemical bonds present in LS fibres with reference to the literature findings are presented in table 4.1.

Table 4.1: Determination of chemical groups present in LS fibre

Plant type wavenumbers (cm^{-1})		**Wavenumber range (cm^{-1})**	**Functional group and Corresponding chemical constitution**	**Reference**
LDTF	**SGF**			
3383	3360	3310 – 3378	Stretching of O-H in alpha cellulose	Maheshwaran [26], Indran [22], Senthamaraikan[38], Maache [44], Belouadah [45]
2918	2918	2800 – 3000	C-H stretching vibration from alpha cellulose	Maheshwaran [26], Babu [18], Indran [22], Senthamaraikannan [38], Maache[44],Belouadah[45]
2362	-	2340 – 2350	C ≡ C stretching presence of waxes	Maheshwaran [26], Senthamaraikannan [38]

Plant type wavenumbers (cm^{-1})		**Wave number range (cm^{-1})**	**Functional group and Corresponding chemical constitution**	**Reference**
LDTF	**SGF**			
1737	1737	1730 – 1760	C = O groups of hemicelluloses	Maheshwaran [26], Senthamaraikannan [38] Belouadah [45]
1634	1635	1635 – 1645	C = O stretching presence of lignin	Senthamaraikannan [38] Belouadah [45]
1510	1510	1510 – 1520	C = C stretching presence of lignin	Maache [44], Belouadah [45]
1425	1425	1418 – 1428	CH_2 symmetric bending of cellulose	Indran [22], Senthamaraikan[38], Maache [44], Belouadah [45]
1376	1374	1371	C-H groups of cellulose	Belouadah [45]
1254	1252	1248	C-O stretching of acetyl group in lignin	Maache [44]
1159	1159	1159	C-O-C groups of cellulose and hemicelluloses	Belouadah [45]
1051	1052	1055	C-O stretching of hydroxyl and ether groups in cellulose	Maache [44]

FTIR spectrum of NaOH extracted LDTF fibre is shown in the Figure 4.21. According to that the peaks belongs to the lignin and waxes were reduced.

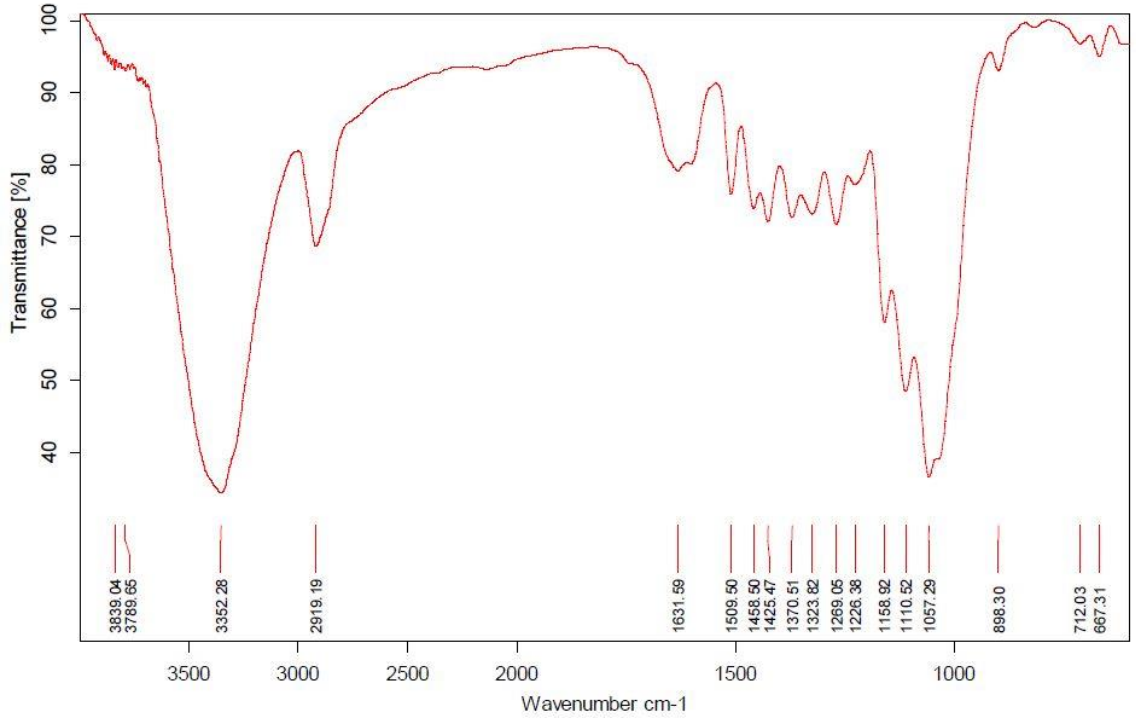

Figure 4.21: FTIR Spectrum of NaOH extracted LDTF

Figure 4.21 clearly indicates the absence of a peak at 2362 cm^{-1} in the NaOH extracted LDTF confirming the removal of waxes during the extraction.

It can be concluded that the LS fibre consists with of cellulose, hemicelluloses, lignin and little amount of wax based on identification of chemical groups by FTIR analysis.

4.4 XRD analysis

Analysis of the fibre structure was performed in Bruker D8 Discover X-Ray Diffractometer. Powdered rhizome fibre samples of both LD and the SG type plants of LS were subjected to X-Ray diffraction and the intensity of radiation diffraction was recorded at 2θ angle with value ranging from 10° - 70° under the settings of 40Kv voltage and 40mA current.

Figure 4.22 shows the X-Ray diffraction pattern of LDTF.

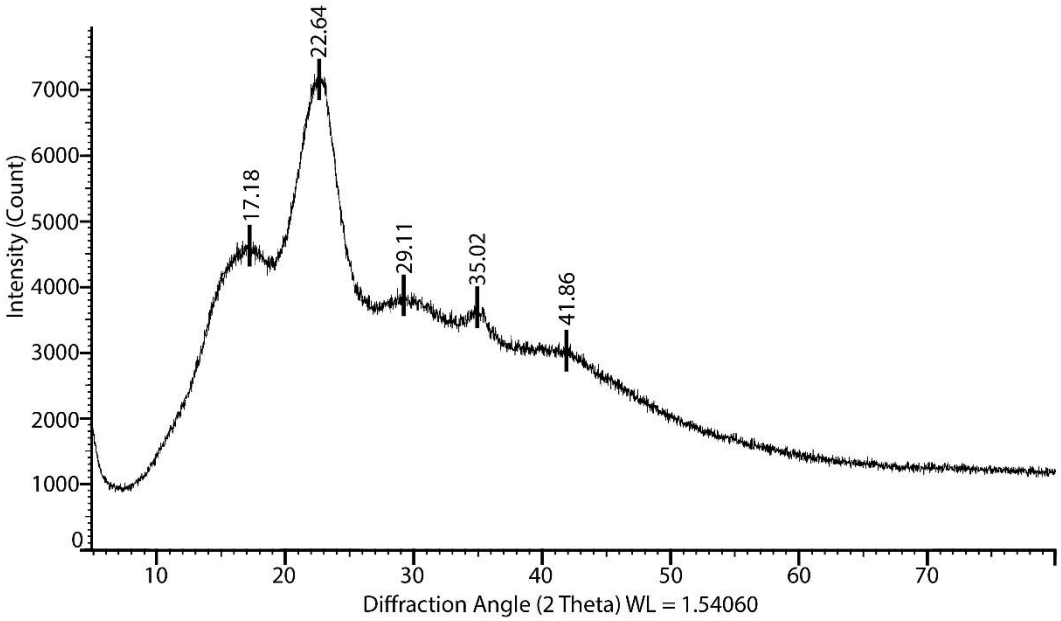

Figure 4.22: X-RD Pattern of LDTF

As suggested by Segal et.al [46], CI calculation was done using the following equation.

$$CI = \left(\frac{I_{002} - I_{am}}{I_{002}}\right)^{0} X\ 100$$

I_{002}, the highest intensity at 2θ = 22.64° corresponds to the peak of the crystalline region and I_{am}, the lowest intensity at 2θ = 17.18° corresponds to the peak of the amorphous region.

Obtained intensity values for the crystalline phase peak, I_{002} and for the amorphous phase peak, I_{am} are presented in table 4.2.

Table 4.2: CI calculation of LDTF

Plant Type	Maximum intensity of crystalline phase peak [I_{002}]	Intensity of the amorphous phase peak [I_{am}]	Crystallinity Index [CI]
Lamina Dissected	6087.51	3481.68	**42.81**

According to the above calculation, CI value of ≅ 43% was obtained for the rhizome fibre extracted LDTF. Table 4.3 presents the CI values of recently researched cellulosic fibres found from different plant sources [21], [22], [26], [31], [38], [39], [45], [47], [48], [49].

Table 4.3: CI of cotton and other cellulosic fibres

Plant and source	Crystallinity index (CI) %	
Cotton seed fibre	60	[21]
Lotus stem fibre	52	[21]
Epipremnum aureum stem fibre	49.33	[26]
Coccinia grandis.L stem fibre	52.17	[38]
Cissus quadrangularis root fibre	56.6	[22]
Althea Officinalis L. stem fibre	65	[39]
Juncus effusus L. stem fibre	33.4	[31]
Date Palm rachis vascular bundles	47.82	[47]
Lygeum spartum L. stem fibre	46.19	[45]
Wrightia tinctoria seed fibre	40.6	[48]
Grewia tiliflia fibre	41.7	[49]

Compared with the CI of the cellulose fibres mentioned in the table 4.3, the CI of LS rhizome fibre is higher than that found in the fibres of *Juncus effusus* L. stem [31], *Wrightia tinctoria* seed [48], *Grewia tiliflia* [49] and is lower than that found in fibres from Cotton seeds [18], lotus stems [21], *Epipremnum aureum* stems [26], *Coccinia*

grandis.L stems [38], *Cissus quadrangularis* roots [22], *Althea Officinalis L*. stems [39], Date Palm rachis vascular bundles [47] and Lygeum spartum L. stems.

The crystal size (Cr_{size}) of the LS fibre was calculated using the Sherrer's equation [18], [30], [35].

$$Cr_{size} = \frac{K\lambda}{\beta \, Cos\theta}$$

Scherrer's constant K = 0.9, wave length of the radiation λ = 1.54 Å [0.154 nm], β is the peak's full width at half maximum [FWHM] while θ is the diffraction angle.

CS calculation of the Lamina Dissected type LS plant rhizome fibre is shown in table 4.4.

Table 4.4: Crystalline Size calculation of LDTF

Peak Position 2θ	**FWHM = β [degrees]**	**Crystalline Size = Kλ / β cosθ [nm]**
22.64	6.35	1.28

The average value of the CS of LDTF is obtained as 1.28nm.

Table 4.5: Crystalline Size of cotton and other cellulosic fibres

Plant and source	**Crystalline Size (nm)**	
Cotton seed fibre	5.5	[43]
Lotus stem fibre	2.5	[20]
Cissus quadrangularis root fibre	28.05	[21]
Coccinia grandis.L stem fibre	13.38	[37]
Epipremnum aureum stem fibre	15	[25]
Juncus effusus L. stem fibre	3.6	[43]

The value obtained for crystal size of the LS fibre is very low compared to those values of fibres of cotton [44], lotus stem [21], *Cissus quadrangularis* root [22], *Coccinia grandis.L* [38], *Epipremnum aureum* [26] and *Juncus effusus L.* [44] fibres.

As stated by Pan et.al [21], fibres with a low degree of crystallinity have lesser amounts of crystal regions and higher percentage of amorphous regions. The CI value of 43% reflects that the LS rhizome fibre consist of higher level of amorphous regions compared to crystalline regions. Further it is [21] stated that the fibres with lower crystallinity levels are with lower strength, higher elongation, greater hygroscopicity and chemical reactivity due to the loose formation of cellulose molecules. Therefore, with the obtained CI and the CS of LS rhizome fibre it can be concluded that the fibre has lower strength, higher elongation, greater hygroscopicity and chemical reactivity. It is known that the plant fibre structures are naturally present to absorb and transport water and nutrients to the other parts of the plant [14].

4.5 Analysis of moisture regain

Rhizome fibres of the two plant types of LS were tested according to the ASTM D2495 - 07 to collect data to measure the moisture content and the moisture regain values of the fibres of each plant type [Appendix A].

4.5.1 Moisture content and regain Calculation

Original mass of the fibre sample

M = Original mass of fibre sample (g)

A = Mass of empty container (g)

B = Gross mass of fibre sample and container (g)

$$M = B - A$$

Oven dry mass of fibre sample

D = Oven-dry mass of fibre sample (g)

C = Oven-dry mass of fibre sample and container (g)

N = Mass of empty container (g)

$$D = C - N$$

Moisture content of the fibre sample

$$\text{Moisture Content \%} = \left(\frac{M - D}{M}\right)^{0} X\ 100$$

Moisture regain of the fibre sample

$$\text{Moisture Regain \%} = \left(\frac{M - D}{D}\right)^{0} X\ 100$$

Calculated moisture content and moisture regain values of both the LDTF and SGF are shown in the Table 4.6 and 4.7.

Table 4.6: Moisture regain and moisture content of LDTF

Sample	[MR] - Moisture Regain %	[MC] - Moisture Content %
1	12.25	10.91
2	11.87	10.61
3	13.07	11.56
4	12.35	10.99
5	13.16	11.63

It can be concluded that moisture content and the moisture regain values of the LDTF as 11.14% and 12.54% respectively.

Table 4.7: Moisture regain and moisture content of SGF

Sample	[MR] - Moisture Regain %	[MC] - Moisture Content %
1	13.24	11.69
2	14.4	12.59
3	16.91	14.47
4	15.93	13.74
5	11.92	10.65

As per the above results and the mean value for moisture content and the moisture regain for SGF are 12.63% and 14.5% respectively. Moisture content and the moisture regain values obtained for both the plant types are shown in table 4.8.

Table 4.8: Comparison of moisture values of LDTF and SGF

Plant Type	**[MR] - Moisture Regain %**	**[MC] - Moisture Content %**
LDTF	12.5	11.4
SGF	14.5	12.63

Table 4.8 indicates that the moisture relationship value as better in SGF than LDTF. This may be due to the presence of wax in the LDTF stand in which it could prevent the penetration of water molecules.

Table 4.9: Cotton and lotus fibre moisture values [50], [51], [37]

Fibre type	**[MR] - Moisture Regain %**	**[MC] - Moisture Content %**
Cotton	7-8	7.34
Lotus	12.32	10.97

The obtained values were compared with moisture content and the moisture regain values of cotton and lotus fibres as given in the in Table 4.9 that indicates the moisture regain and moisture content values obtained for LDTF and SGF are comparatively higher than that the values found for the cotton and lotus fibre. This may be possible due to the higher amorphous content in the LS fibre.

4.6 Tensile Test of LS fibres

4.6.1 Linear density of the fibres

Linear density of the LDTF and SGF calculated according to the ASTM D1577-07 are shown in table 4.10.

Table 4.10: Linear density calculation of LDTF and SGF

Fibre type	Tex
LDTF	0.75
SGF	0.76

Both the types of LS fibre linear density obtained through mechanical extraction method were similar.

4.6.2 Tensile behavior of fibres

Figure 4.23 and 4.24 illustrate the load extension graphs obtained for LDTF and SGF respectively according to ASTM D3822-14 standard at a constant rate of extension of 10mm/min. The shapes of the graphs are very similar to the load-elongation graph of a crimpy fibre. In this curve, de-crimping of the fibre, deformation, yield point and sudden drop of tension at the breaking point are clearly recorded.

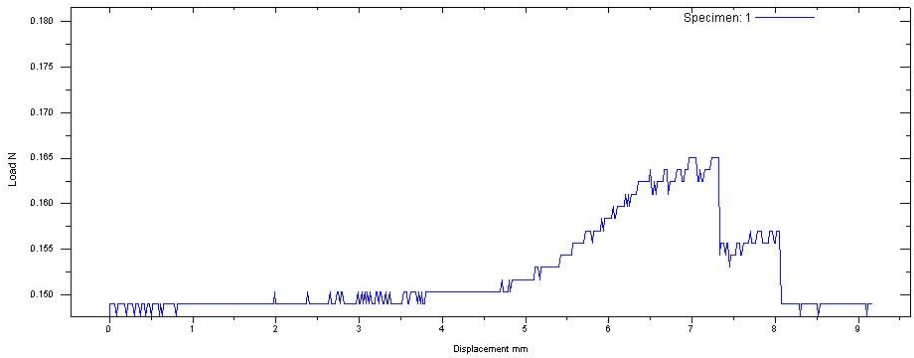

Figure 4.23: LDTF fibre tensile behaviour

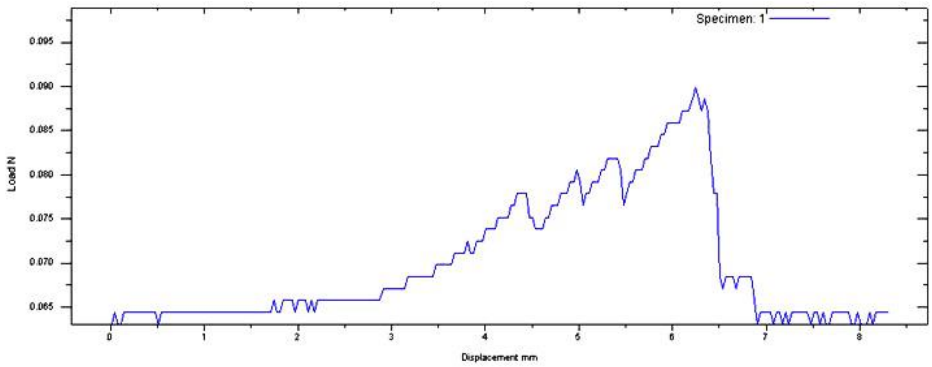

Figure 4.24: SGF fibre tensile behaviour

Both the above graphs show a similar pattern with initial de-crimping, secondary deformation, yield point and sudden drop of tension due to fibre break. According to Booth [54], elongation at the beginning of deformation stage is due to stretch and shear of the primary and secondary bonds of the amorphous phases.

4.6.3 Tensile strength

The tensile strength of both the LS fibres were calculated by testing 30 samples each at indicated values of force at break [Appendix B and C]. Graphs were plotted with indicated breaking load values for both the fibres to understand the distribution of load on tested fibre samples [Appendix D]. A scattering of load at break of individual fibres of both the plant types were observed.

According to the tensile strength values obtained, LDTF and SGF are having approximately 205 MPa and 201 MPa respectively. The tensile strength values obtained for LS fibres are compared with values given in literature findings presented in table 4.11.

Table 4.11: Tensile strength values of plant fibres

Plant and source	**Tensile strength (MPa)**	
Cotton - seed	400	[22]
Lygeum spartum L. – stem	280	[45]
Cissus quadrangularis - root	1857 – 5330	[22]
Coccinia grandis.L - stem	273 ± 27.74	[38]
Epipremnum aureum - stem	317 -810	[26]
Pineapple – Leaf	126.6	[53]
Juncus effusus L. - stem	113 ± 36	[44]
Flax - stem	500 – 1500	[22]
Jute – stem	393 – 773	[22]
Banana – stem	529 – 759	[22]
Althaea officinalis L. – stem	415.2	[38]

According to the table 4.11, cotton fibre tensile strength is higher than that obtained for the LDTF and SGF. Further the LS fibre tensile strength is higher than the values that are reported for Pineapple leaf fibre and *Juncus effusus L.* [44] and lower than *Lygeum spartum* L. [45], *Cissus quadrangularis* [22], *Coccinia grandis.L* [38], Flax [22], Jute [22], Banana [22], *Althaea officinalis* L. [38]. The tensile strength of [26], which belongs to the same plant family as LS, indicated a higher value, proving that same plant family fibre can have different strength values.

The differences of fibre breaking load for tested fibres may result mainly due to the variations in the count of fibrils in test specimens. Formation differences in individual fibres such as age or maturity and growing conditions would have influenced as well [45]. As the results obtained from the SEM analysis, X-RD analysis and FTIR analysis, it is confirmed that the two fibre types are almost similar in its morphology, crystallinity index and the chemical composition. This may be the reason for the occurrence of similar tensile values for both the fibre types.

4.6.4 Breaking elongation

When load is applied to individual fibres, it is observed that the fibres stretch up to a certain extent. Elongation values for each fibre were calculated as per the standard. Graphs were plotted with the calculated elongation values [Appendix A, B and E] of each tested sample.

The mean value of the extension of LDTF and SGF are 16.89% and 16.94%. As per the above results, the strain at break percentage value of both the fibre types are very similar. Elongation percentage values found for cotton fibre and several other cellulosic fibres are presented in table 4.12.

Table 4.12: Elongation percentage values of cotton and other plant fibres

Plant and source	**Elongation (%)**	
Cotton - seed	7-8	[22]
Jute – stem	1.15 -1.5	[44]
Hemp – bast	2.2	[44]
Epipremnum aureum – stem	1.38 -4.2	[26]
Cissus quadrangularis - root	3.57 – 8.37	[22]
Bamboo	1.4	[22]
Banana	1 -3.5	[22]

As per the findings in table 4.12, LS fibre elongation percentage is higher than Cotton [22], Jute [44], Hemp [44], *Epipremnum aureum* [26], *Cissus quadrangularis* [22], Bamboo [22] and Banana [22] fibres.

According to above literature findings it is clearly evident that the elongation of LS is higher than that of the most common and recently investigated fibres. Further as confirmed by XRD results, LS fibre consist with more amorphous regions than crystalline regions. As reported by Booth [54], orderly arranged long chain molecules lead to the formation of crystalline regions are lesser and long chain molecules that are organized in haphazard manner lead to the formation of the amorphous regions. As stated previously deformation of high amorphous region and the less crystalline regions result the higher extension percentage of LS fibres.

4.6.5 Young's modulus

Young's modulus of both the LDT and SG fibres are obtained as 1.3 GPa. Young's modulus values of Cotton and other cellulosic are presented in table 4.13.

Table 4.13: Young's modulus of cotton and plant fibres

Plant and source	**Young's modulus (**GPa**)**	
Cotton - seed	5 -12	[22]
Flax – stem	52.5 ± 8.6	[44]
Jute – stem	1.3 – 42.2	[44]
Epipremnum aureum - stem	8.41– 69.61	[26]
Cissus quadrangularis	68 – 203	[22]

When comparing the Young's modulus value of the LS fibre with the values of cotton and other cellulosic fibres in table 4.13, it is clearly evident that the LS fibre has lower modulus than Cotton, Flax, Jute, *Epipremnum aureum* and *Cissus quadrangularis* fibres. According to Booth [54], the Young's modulus indicate the force required to produce a small extension. Therfore the high modulus indicates less stretchability and a low modulus indicates great stretchability. With the obtained Young's modulus results for the LS fibre, it can conclude that the fibre has higher extensibility during the initial stage of application of stress.

4.7 Dye up-take behavior of LS

The reflectance value at all wavelengths of dyed LS textile samples of both the LDTF and the SGF were measured using a Datacolor 800 Spectrophotometer. The light reflectance (R) values of the dyed textile samples at the maximum weave length of absorbency (λ maximum) were observed and graphs were plotted.

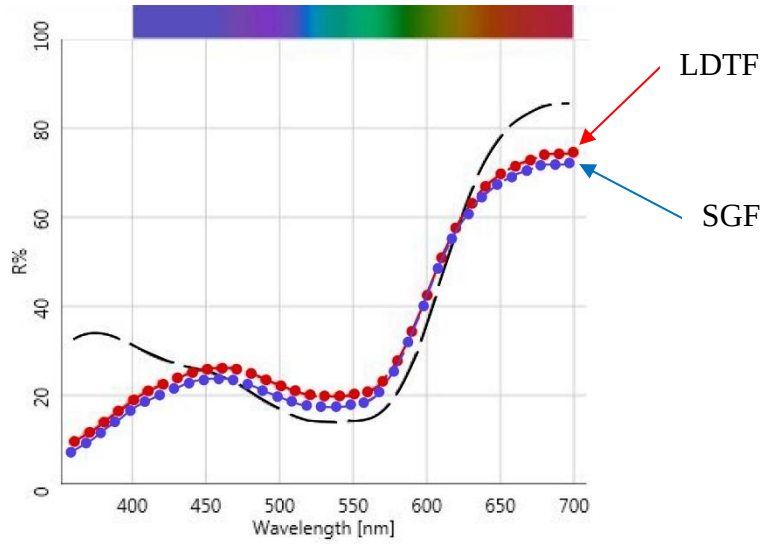

Figure 4.25: Light reflectance (R) values vs wavelength of LDTF and SGF

Colour strength (K/S) of both the LS textile samples and the cotton textile sample were calculated using the Kubelka – Munk theory and the equation mentioned below.

K = Absorption Coefficient

S = Scattering Coefficient

$$K/S = \frac{(1 - R)^2}{2R}$$

The obtained test results of the light reflectance values at the maximum wave length range of 700 – 750 nm for each dyed textile samples are as in table 4.14.

Table 4.14: Light reflectance and colour strength values

Fibre type	**Light reflectance value (R)**	**Colour strength (K/S)**	
LDTF	73.79	35.9	
SGF	73.58	35.8	
Cotton	85.62	41.8	[54]

According to the above results for the colour strength of LDTF, SGF and Cotton fibre, with respect to the reactive dyes in to each of the fibre types, it is identified that the dye

absorbency of the LS rhizome fibres were lower than that to Cotton fibres. However, the two types of LS rhizome fibres shows almost similar dye uptake behavior.

The lower dye uptake of LS fibres compared to cotton may be due to the presence of lignin and other non-cellulosic material in LS fibre

4.8 Thermo gravimetric Analysis

The thermogravimetric (TG) and its derivative thermogravimetric (DTG) curves obtained for the LDTF and SGF are shown in Figure 4.26 and Figure 4.27 respectively.

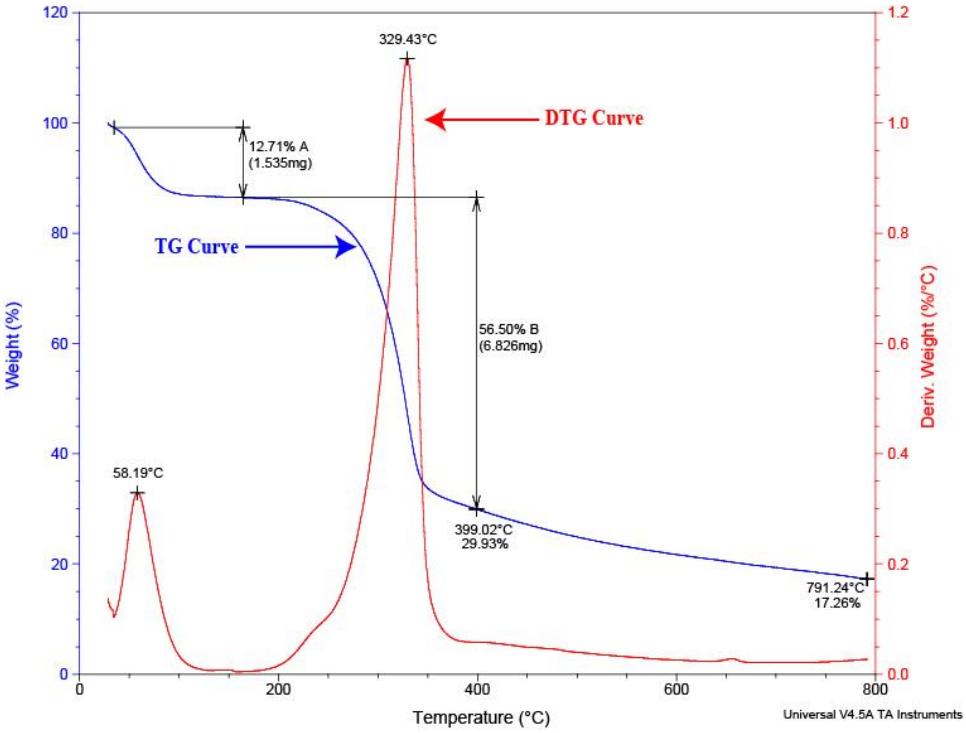

Figure 4.26: TG and DTG Curves of LDTF

According to the TG curve shown in Figure 4.26, the initial weight loss of 12.71% occurred in between the room temperature and 100℃. This weight loss is due to the vaporization of water present in the fibre which is similar to the observations of Maheshwaran et al. [26].

After the initial mass loss, it is observed a region of thermal stability from 100℃ to 230℃. The second mass loss is observed between 230℃ to 340℃. According to several research

findings [22], [26], [38], [39] this result obtained for the LS fibre corresponds to the glycosidic linkages of cellulose and breakdown of hemicelluloses in fibre. The derivative thermogravimetry (DTG) curve shows a clear peak at 329.43℃ and it is considered as the decomposition peak temperature which indicates the thermal decomposition of cellulose I and complete decomposition of ∝-cellulose.

As found in literature the third stage of the TG spectrum indicates the degradation of wax and lignin of the LS fibre within the temperature range of 340℃ - 500℃ [17], [22], [38]. According to the FTIR spectrums shown in Figure 4.19 and 4.20, it is found that the LS rhizome fibre consist of small quantities of Lignin and waxes. Therefore, the weight loss recorded in the spectrum of LDTF is attributed to the degradation of wax and lignin in the LS fibre.

As reported in the literature [22] at temperature above 500℃, the molecules of the fibre will breakdown into CO_2, CO, H_2O, hydrocarbons and hydrogen which are low molecular weight products.

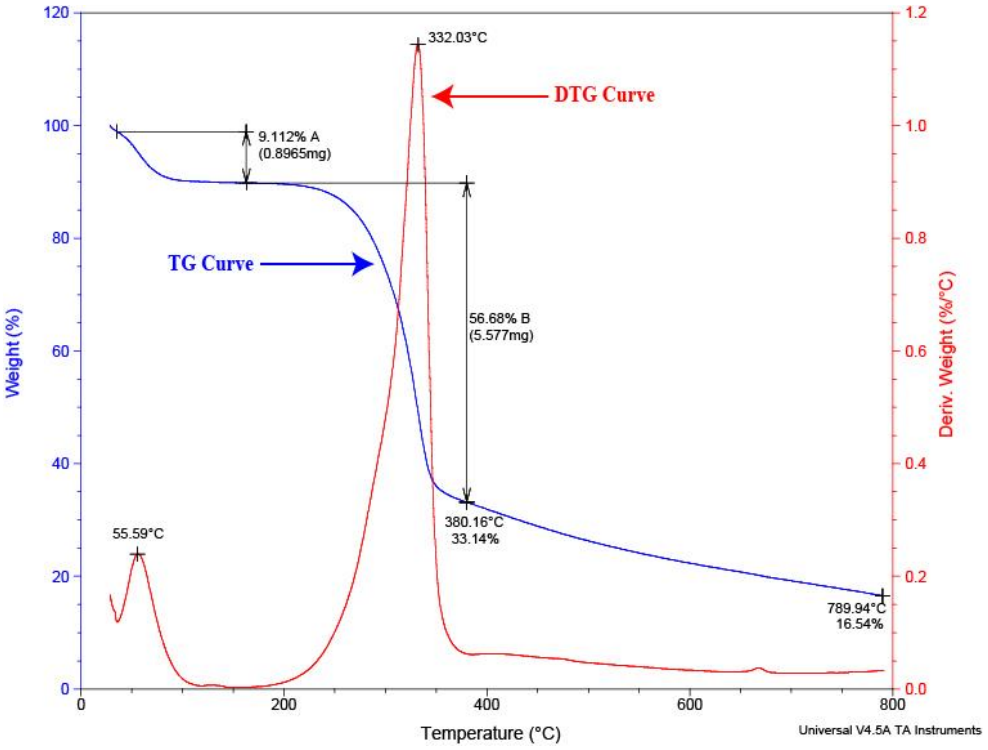

Figure 4.27: TG and DTG Curves of SGF

The thermal behavior of the SGF indicates the initial weight loss within the temperature range of ambient to100℃. The second mass loss is also observed at the temperature range of 230℃ to 340℃, confirming similar thermal behavior to the LDTF. However according to the DTG curve, the decomposition peak temperature of SGF shows as 332.03℃ and that is slightly higher than the peak temperature of 329.43℃, obtained for the LDTF, which is attributed to the thermal decomposition of cellulose I and complete decomposition of ∝-cellulose. Similar peaks are recorded in the literature for several natural fibres such as Bamboo, Hemp, Jute and Kenaf fibres at 321℃, 308.2℃, 298.2℃ and 307.2℃ respectively [22].

The results of the thermal analysis of both fibre types indicate that the raw LS fibre has thermal stability up to 230℃. Indicating that the LS fibre can withstand most of the textile process conditions and it is possible to be use the LS fibre in manufacture of composites.

CHAPTER 5: CONCLUSION AND RECOMMENDATIONS

This research presents the characterization of *Lasia spinosa* (L.) Thwaites rhizome fibre extracted from two commonly available species in Sri Lanka, which are called Lamina dissected and Sagittate plants, identified according to its leaf shape to evaluate their potential use as a biodegradable textile material. The morphological characteristics, chemical functional groups, crystallinity, tensile properties, thermal stability, moisture absorbency and dye up take of the fibre were investigated in order to create a knowledge base to be used in manufacturing textile of material. Fibres were extracted by mechanical extraction and alkali extraction methods from well grown rhizomes in equal age of both the plant types which were collected from farmers in the Western province of Sri Lanka

The morphological characterization of fibres from both the plant types reveals that the LS rhizome contains approximately 100 -120 fibre bundles as vascular bundles which are running through the rhizome. These bundles consist with 4-5 fibres with diameter in the range of 31 μm – 47 μm. Each fibre contains approximately 16 – 25 fibrils with a diameter range of 2.5 μm – 6.5 μm. Loose structure of fibril bundles gives a fluffy formation to fibres. It is observed that the mechanically extracted fibres are with inherent crimp and that contributes to the elasticity of fibres. It is identified that the crimp on these fibres are more like the crimp on wool fibres. In comparison with Cotton fibre morphology, crimp on these fibres is a unique feature for LS fibre.

Chemical nature of fibre was investigated through FTIR and the X-RD testing. The FTIR analysis of fibre from both plant types confirmed that they consist with cellulose, hemicelluloses, lignin and small amount of waxes as found in other plant fibres. NaOH extracted fibres showed a lower level of lignin and waxes. Both the fibre types showed slight differences in transmittance values.

The X-RD analysis confirmed the presence of high amorphous percentage and low crystal percentage. Crystallinity index value of 43% was obtained and in comparison, with the crystallinity value of 63.59% cotton, it is confirmed that the LS fibres are having a low amount of crystal phases and higher amount of amorphous regions than cotton fibre.

Calculated crystalline size of 1.28nm for LS fibre is lower than the 5.5nm value of cotton fibre.

Moisture regain and moisture content values of two plant type fibres showed slight differences, resulting 12.54% and 11.14% for LD fibre and 14.5% and 12.63% for SG fibre respectively. Compared to LD fibre, SG fibre has higher moisture absorbency and moisture content. In comparison with cotton moisture regain value of 7-8% and 7.34% of moisture content it is confirmed that the LS fibre has higher moisture regain and moisture content values.

The tensile strength of fibre was obtained as 205 MPa for LD fibre and 201 MPa for Sagittate fibre which are lower than that of cotton fibre value of 400 MPa as found in literature. Very high breaking elongation was obtained for both the fibre types giving 16.89% and 16.94% for LD and SG fibres respectively in comparison to breaking elongation value of 7-8% for cotton. The obtained Young's modulus for both LS fibre types are 1.26 GPa for LD and 1.18GPa for SG respectively. Compared to cotton fibre Young's modulus of 5 -12 GPa, LS shows a lower value indicating higher extensibility under with small extensions.

Dye up take behavior of LS fibre was analyzed obtaining the light reflectance value of 73.79 for LD and 73.58 for SG. The results obtained for both fibre types are lower than that of cotton fibre value of 85.62. Colour strength (K/S) values of both LS fibre types shown similar but lower than the cotton K/S value of 41.8 confirming that the dye absorbency of the LS fibre is lower than cotton fibres.

The thermal stability of both the fibre types were obtained from the thermo gravimetric curves of respective fibres and confirmed that LS fibres have thermal stability up to 230℃ indicating that the fibre can withstand most of the textile processing conditions and possible to be used in manufacturing of composites.

All above fibre characterization investigation of fibre properties such as fibre crimp, lower count, higher elongation, greater moisture absorbency, moisture content and dye

absorbency and good thermal stability indicate the possible use of LS fibre for manufacture of biodegradable textile materials. As the LS plant is known as a herbal plant that uses all the parts of the plant in Ayurvedic medicines as a cure for many ailments, possibilities are there to develop medicinal textiles with LS fibre. Therefore, as future work it is suggested to investigate the hydrophilicity, nontoxicity and antimicrobial characteristics of the LS rhizome fibre find out the possibilities in medicinal applications.

The high amorphous content of LS fibre may make it possible to be used as an alternative medicine to absorb unwanted microorganisms or foreign matter inside the digestive system of humans similar to Kaolin tablets. As the cellulose fibres are already used by the pharmaceutical industry to manufacture wound care products and implant materials for human body, opportunities are available to focus the future research work on these areas as well.

REFERENCES

[1] R.S.Blackburn. (2005). *Biodegradable and sustainable fibres.* Cambridge: Woodhead Publishing Limited.

[2] K. Fletcher, "Sustainable Fashion and Textiles", *ResearchGate*, 2012. Available: 10.4324/9781849772778.

[3] S. Muthu, *Sustainable Innovations in Textile Fibres*. Springer Singapore, 2018.

[4] S. MIshra, *Fibre Structure*, 1st ed. New Delhi: WPI India, 2016.

[5] H.Wardman, R. R. (2015). *The Chemistry of Textile Fibres.* Cambridge: Royal Society of Chemistry,UK.

[6] A. Parry, "Nanocellulose and its Composites for Biomedical Applications", *ResearchGate*,2016.[Online].Available:https://www.researchgate.net/publication/309350498_Nanocellulose_and_its_Composites_for_Biomedical_Applications.

[7] A. Dumanlı and A. Windle, "Carbon fibres from cellulosic precursors: a review", *SpringerLink*,2020.[Online].Available:https://link.springer.com/article/10.1007%2Fs10853-011-6081-8#citeas.

[8] D. Miyashiro, R. Hamano and K. Umemura, "A Review of Applications Using Mixed Materials of Cellulose, Nanocellulose and Carbon Nanotubes", *ResearchGate*,2020.[Online].Available:https://www.researchgate.net/publication/338723603_A_Review_of_Applications_Using_Mixed_Materials_of_Cellulose_Nanocellulose_and_Carbon_Nanotubs.

[9] D. Trache, M. Hussin, M. Haafiz and V. Thakur, "Recent progress in cellulose nanocrystals: sources and production", *Nanoscale*, vol. 9, no. 5, pp. 1763-1786, 2017. Available: 10.1039/c6nr09494e.

[10] U. Kankanamge and D. Amarathunga, "PHYTOCHEMICAL AND ETHNO-PHARMACOLOGICAL PROPERTIES OF LASIA SPINOSA (KOHILA): A REVIEW", *World Journal of Pharmaceutical Research*, vol. 6, no. 13, pp. 1-9, 2017. Available: DOI: 10.20959/wjpr201713-9837.

[11] T.Kumari, R.Rajapaksha, L.Karunarathne, G.Pushpakumara, P.Bandaranayake, et al., “Morphological characterization of *Lasia spinosa* (L.) Thw.: Screening of indigenous crop genetic resources for future food and nutritional security”, *Sri Lanka Journal of Food and Agriculture*, pp.31, Dec 2017.

[12] H. Puspita, "Studies on karyomorphology and in vitro propagation of *lasia spinosa* thwaites", Ph.D, Gauhati University, 2015.

[13] S. Mayo, J. Bogner and P. Boyce, "THE GENERA OF ARACEAE PROJECT", *Curtis's Botanical Magazine*, vol. 12, no. 3, pp. 125-126, 1995. Available: 10.1111/j.1467-8748. 1995.tb00500. x.

[14] E. McHenry, *Botany in 8 lessons*. State College, PA: Ellen McHenry's Basement Workshop, 2013, pp. 27-29.

[15] F. Essig, "Everything you wanted to know about plant cells, but were afraid to ask", *Botany Professor*, 2015.

[16] L. Baessler, "What Is A Rhizome: Learn About Rhizome Plant Facts", *Gardening Know How*, 2018. [Online]. Available: https://www.gardeningknowhow.com/ornamental/bulbs/bgen/what-is-a-rhizome.htm.

[17] K. Murugesh Babu, M. Selvadass & R. Somashekar (2013) Characterization of the conventional and organic cotton fibres, *Journal of The Textile Institute*, 104:10, 1101-1112, DOI:10.1080/00405000.2013.774948

[18] M. Fan, D. Dai and B. Huang, "Fourier Transform Infrared Spectroscopy for Natural Fibres", *Fourier Transform - Materials Analysis*, pp. 46-62, 2012. Available: 10.5772/35482 [Accessed 11 April 2020].

[19] TASNIM N. SHAIKH, S. A. AGRAWAL, "Qualitative and Quantitative Characterization of Textile Material by Fourier Transform Infra-Red," *IJIRSET*, vol. 3, no. 1, January 2014, pp. 8496,8497,8498, 2014.

[20] Z. Belouadah, A. Ati, M. Rokbi, "Characterization of new natural cellulosic fibre from *Lygeum spartum* L.," *Carbohydrate Polymers*, vol. 134, no. 2015, p. 429–437, 2015.

[21] Y. Pan et al., "Structural characteristics and physical properties of lotus fibres obtained from Nelumbo nucifera petioles", *Carbohydrate Polymers*, vol. 85, no. 1, pp. 188-195, 2011. Available: 10.1016/j.carbpol.2011.02.013.

[22] S.Indran, R.Edwin Raj, V.S.Sreenivasan, "Characterization of new natural cellulosic fibre from *Cissus quadrangularis* root," *Carbohydrate Polymers*, vol. 110, no. 22 September 2014, pp. 423-429, 2014.

[23] C. Cheng et al., "Preparation and characterization of lotus fibres from lotus stems", *The Journal of The Textile Institute*, vol. 109, no. 10, pp. 1322-1328, 2018. Available: 10.1080/00405000.2018.1423898.

[24] S. Sadi and J. Hossain, "Measurement of the relationship between shade (%), reflectance (%) and color strength (K/S)", *Textile News, Apparel News, RMG News, Fashion Trends*, 2020.

[25] M. Abate and V. Nierstrasz, "Combined Pre-Treatment and Causticization of Cotton Fabric for Improved Dye Uptake", *Advance Research in Textile Engineering*, vol. 2, no. 1, 2017. Available: 10.26420/advrestexteng.2017.1016.

[26] M. Maheshwaran, N. Hyness, P. Senthamaraikannan, S. Saravanakumar and M. Sanjay, "Characterization of natural cellulosic fibre from *Epipremnum aureum* stem", *Journal of Natural Fibres*, vol. 15, no. 6, pp. 789-798, 2017. Available: 10.1080/15440478.2017.1364205.

[27] S. Arju, A. Afsar, D. Das and M. Khan, "Role of Reactive Dye and Chemicals on Mechanical Properties of Jute Fabrics Polypropylene Composites", *Procedia Engineering*, vol. 90, pp. 199-205, 2014. Available: 10.1016/j.proeng.2014.11.837.

[28] E. Portella, D. Romanzini, C. Angrizani, S. Amico and A. Zattera, "Influence of Stacking Sequence on the Mechanical and Dynamic Mechanical Properties of Cotton / Glass Fiber Reinforced Polyester Composites", *Materials Research*, vol. 19, no. 3, pp. 542-547, 2016. Available: 10.1590/1980-5373-mr-2016-0058.

[29] R. Kozlowski, *Handbook of natural fibres*. Cambridge: Woodhead Publishing Ltd, 2012.

[30] P. Wakelyn, *Cotton fibre chemistry and technology*. Boca Raton: CRC Press, 2007.

[31] G. Chinga-Carrasco, "Cellulose fibres, nanofibrils and microfibrils: The morphological sequence of MFC components from a plant physiology and fibre technology point of view", *Nanoscale Research Letters*, vol. 6, no. 1, 2011. Available: 10.1186/1556-276x-6-417.

[32] P. Garside and P. Wyeth, "Identification of Cellulosic Fibres by FTIR Spectroscopy - Thread and Single Fibre Analysis by Attenuated Total Reflectance", *Studies in Conservation*, vol. 48, no. 4, pp. 269-275, 2003. Available: 10.1179/sic.2003.48.4.269.

[33] M. Sfiligoj, S. Hribernik, K. Stana and T. Kree, "Plant Fibres for Textile and Technical Applications", *Advances in Agrophysical Research*, 2013. Available: 10.5772/52372.

[34] C.Yu, "NATURAL TEXTILE FIBRES: VEGETABLE FIBRES," in *TEXTILES AND FASHION*, Shanghai, Elsevier Ltd., 2015, p. 34.

[35] Y. Liu, D. Thibodeaux and J. Rodgers, "Preliminary Study of Linear Density, Tenacity, and Crystallinity of Cotton Fibres", *Fibres*, vol. 2, no. 3, pp. 211-220, 2014. Available: 10.3390/fib2030211.

[36] R. Pandey, M. Sinha and A. Dubey, "Cellulosic fibres from Lotus (Nelumbo nucifera) peduncle", *Journal of Natural Fibres*, vol. 17, no. 2, pp. 298-309, 2018. Available: 10.1080/15440478.2018.1492486.

[37] D. Chen, Y. Gan and X. Yuan, "Research on Structure and Properties of Lotus Fibres", *Advanced Materials Research*, vol. 476-478, pp. 1948-1954, 2012. Available: 10.4028/www.scientific.net/amr.476-478.1948.

[38] P. Senthamaraikannan and M. Kathiresan, "Characterization of raw and alkali treated new natural cellulosic fibre from *Coccinia grandis.L*", *Carbohydrate Polymers*, vol. 186, pp. 332-343, 2018. Available: 10.1016/j.carbpol.2018.01.072.

[39] A. KılınÇ, S. Köktaş, M. Atagür and M. Seydibeyoglu, "Effect of Extraction Methods on the Properties of Althea Officinalis L. Fibres", *Journal of Natural Fibres*, vol. 15, no. 3, pp. 325-336, 2017. Available: 10.1080/15440478.2017.1325813.

[40] C. Cheng, R. Guo, J. Lan and S. Jiang, "Extraction of lotus fibres from lotus stems under microwave irradiation", *Royal Society Open Science*, vol. 4, no. 9, p. 170747, 2017. Available: 10.1098/rsos.170747.

[41] J. Kim et al., "Review of nanocellulose for sustainable future materials" , *International Journal of Precision Engineering and Manufacturing-Green Technology*, vol. 2, no. 2, pp. 197-213, 2015. Available: 10.1007/s40684-015-0024-9.

[42] H. Kim, K. Okubo, T. Fujii and K. Takemura, "Influence of fibre extraction and surface modification on mechanical properties of green composites with bamboo fibre", *Journal of Adhesion Science and Technology*, vol. 27, no. 12, pp. 1348-1358, 2013. Available: 10.1080/01694243.2012.697363.

[43] R. Wahab, A. Mohamed, M. Mustafa and A. Hassan, "Physical Characteristics and Anatomical Properties of Cultivated Bamboo (Bambusa vulgaris Schrad.) Culms", *Journal of Biological Sciences*, vol. 9, no. 7, pp. 753-759, 2009. Available: 10.3923/jbs.2009.753.759.

[44] M. Maache, A. Bezazi, S. Amroune, F. Scarpa and A. Dufresne, "Characterization of a novel natural cellulosic fibre from *Juncus effusus* L.", *Carbohydrate Polymers*, vol. 171, pp. 163-172, 2017. Available: 10.1016/j.carbpol.2017.04.096.

[45] Z. Belouadah, A. Ati and M. Rokbi, "Characterization of new natural cellulosic fibre from Lygeum spartum L.", *Carbohydrate Polymers*, vol. 134, pp. 429-437, 2015. Available: 10.1016/j.carbpol.2015.08.024.

[46] L. Segal, J. Creely, A. Martin and C. Conrad, "An Empirical Method for Estimating the Degree of Crystallinity of Native Cellulose Using the X-Ray Diffractometer", *Textile Research Journal*, vol. 29, no. 10, pp. 786-794, 1959. Available: 10.1177/004051755902901003.

[47] H. Boumediri, A. Bezazi, G. Del Pino, A. Haddad, F. Scarpa and A. Dufresne, "Extraction and characterization of vascular bundle and fibre strand from date palm rachis as potential bio-reinforcement in composite", *Carbohydrate Polymers*, vol. 222, p. 114997, 2019. Available: 10.1016/j.carbpol.2019.114997.

[48] K. Subramanian, P. Senthil Kumar, P. Jeyapal and N. Venkatesh, "Characterization of ligno-cellulosic seed fibre from Wrightia Tinctoria plant for textile applications—an exploratory investigation", *European Polymer Journal*, vol. 41, no. 4, pp. 853-861, 2005. Available: 10.1016/j.eurpolymj.2004.10.037.

[49] J. Jayaramudu, B. Guduri and A. Varada Rajulu, "Characterization of new natural cellulosic fabric Grewia tilifolia", *Carbohydrate Polymers*, vol. 79, no. 4, pp. 847-851, 2010. Available: 10.1016/j.carbpol.2009.10.046.

[50] K. Jegatheesan, "Feasibility study on the utilization of lotus fibres as a textile raw materials", *Dl.lib.mrt.ac.lk*, 2019.

[51] R. Sohel, "Standard Moisture Regain and Moisture Content of Fibres", *Textilecalculation.blogspot.com*, 2015. [Online]. Available: https://textilecalculation.blogspot.com/2015/08/standard-moisture-regain-and-moisture.html.

[52] J. McKittrick, P. Chen, S. Bodde, W. Yang, E. Novitskaya and M. Meyers, "The Structure, Functions, and Mechanical Properties of Keratin", *JOM*, vol. 64, no. 4, pp. 449-468, 2012. Available: 10.1007/s11837-012-0302-8.

[53] R. Arib, S. Sapuan, M. Ahmad, M. Paridah and H. Zaman, "Mechanical properties of pineapple leaf fibre reinforced polypropylene

composites", *Materials & Design*, vol. 27, no. 5, pp. 391-396, 2006. Available: 10.1016/j.matdes.2004.11.009.

[54] J. Booth, *Principles of textile testing*, 1st ed. London: Butterworths, 1986.

[55] M. Hossen and Imran, "Study on Color Strength of Different Reactive Dyes", *Journal of Textile Science & Engineering*, vol. 07, no. 02, 2017. Available: 10.4172/2165-8064.1000293.

Appendix A

Amount of moisture calculation in LDTF

Sample	[A] - Mass of Empty Container (g)	[B] – Mass of Fibre sample & Container (g)	[C] – Gross Mass of Oven dried fibre sample & Container (g)	[M] - Sample Weight (g)	[D] - Oven Dry Weight of Sample (g)	Weight of Water in sample (g)
1	151.895	157.247	156.663	5.352	4.768	0.584
2	152.532	157.933	157.36	5.401	4.828	0.573
3	152.592	157.983	157.36	5.391	4.768	0.623
4	153.231	158.627	158.034	5.396	4.803	0.593
5	151.890	157.291	156.662	5.4	4.772	0.629

Amount of moisture calculation in SGF

Sample	[A] - Mass of Empty Container (g)	[B] – Mass of Fibre sample & Container (g)	[C] – Gross Mass of Oven dried fibre sample & Container (g)	[M] - Sample Weight (g)	[D] - Oven Dry Weight of Sample (g)	Weight of Water in sample (g)
1	151.895	152.895	156.805	5.56	4.91	0.65
2	152.532	154.532	157.322	5.48	4.79	0.69
3	151.895	154.895	156.471	5.35	4.576	0.774
4	151.9	155.9	156.67	5.53	4.77	0.76
5	152.538	157.538	157.488	5.54	4.95	0.59

Appendix B

LDTF Tensile data and calculations

Lamina Dissected Type Fibre Tensile Testing Data								
Machine speed	**Sample Number**	**Load N**	**Lamina Tex count**	**Lamina Tensile strength / Tenacity (N/Tex)**	**Lamina Tensile strength / Tenacity (MPa)**	**Extension mm**	**Strain at Break (ε) %**	**Young's modulus [E]**
10mm/min	1	0.1544	0.75	0.21	205.87	7.57	15.14	1.36
10mm/min	2	0.1476	0.75	0.19	196.8	13.74	27.48	0.72
10mm/min	3	0.1664	0.75	0.22	221.87	7.29	14.58	1.52
10mm/min	4	0.1812	0.75	0.24	241.6	8.46	16.92	1.43
10mm/min	5	0.1195	0.75	0.16	159	6.28	12.56	1.27
10mm/min	6	0.1546	0.75	0.21	206.13	7.79	15.58	1.32
10mm/min	7	0.1732	0.75	0.23	230.93	10.97	21.94	1.05
10mm/min	8	0.1652	0.75	0.22	220.26	7.71	15.42	1.43
10mm/min	9	0.1821	0.75	0.24	242.8	9.16	18.32	1.32
10mm/min	10	0.1316	0.75	0.17	160	9.41	18.82	0.93
10mm/min	11	0.1541	0.75	0.20	205.47	9.09	18.18	1.13
10mm/min	12	0.1537	0.75	0.20	204.93	6.28	12.56	1.63
10mm/min	13	0.1726	0.75	0.23	230.13	6.24	12.48	1.84
10mm/min	14	0.1543	0.75	0.20	205.73	8.65	17.3	1.19
10mm/min	15	0.1616	0.75	0.21	161	9.84	19.68	1.09
10mm/min	16	0.1731	0.75	0.23	230.8	9.15	18.3	1.26
10mm/min	17	0.1593	0.75	0.21	212.4	10.2	20.4	1.04
10mm/min	18	0.1824	0.75	0.24	243.2	7.34	14.68	1.66
10mm/min	19	0.1482	0.75	0.19	197.6	8.14	16.28	1.21
10mm/min	20	0.1478	0.75	0.19	162	9.64	19.28	1.02
10mm/min	21	0.1673	0.75	0.22	223.06	7.74	15.48	1.44
10mm/min	22	0.1274	0.75	0.17	169.86	9.04	18.08	0.94
10mm/min	23	0.1937	0.75	0.26	258.26	8.95	17.9	1.44
10mm/min	24	0.1688	0.75	0.22	225.06	6.32	12.64	1.78
10mm/min	25	0.1533	0.75	0.20	163	7.16	14.32	1.43
10mm/min	26	0.1546	0.75	0.21	206.13	9.29	18.58	1.10
10mm/min	27	0.1353	0.75	0.18	180.4	8.94	17.88	1.00
10mm/min	28	0.1667	0.75	0.22	222.26	6.4	12.8	1.74
10mm/min	29	0.1582	0.75	0.21	210.93	7.34	14.68	1.44
10mm/min	30	0.1449	0.75	0.19	164	9.25	18.5	1.04
Average Strength and Strain					**205.38 MPa**		**16.89%**	**1.29**

Appendix C

SGF Tensile data and calculations

Sagittate Type Fibre Tensile Testing Data								
Machine speed	**Sample Number**	**Load N**	**SG Tex**	**SG Tensile strength / Tenacity (N/Tex)**	**Lamina Tensile strength / Tenacity (MPa)**	**Extension mm**	**Strain at Break (ε) %**	**Young's modulus [E]**
10mm/min	1	0.1409	0.76	0.18	185.39	5.92	11.84	1.56
10mm/min	2	0.1603	0.76	0.21	210.92	13.6	27.2	0.77
10mm/min	3	0.1376	0.76	0.18	181.05	8.65	17.3	1.05
10mm/min	4	0.1298	0.76	0.17	170.79	9.84	19.68	0.87
10mm/min	5	0.1571	0.76	0.21	206.71	9.15	18.3	1.13
10mm/min	6	0.1559	0.76	0.21	205.13	10.2	20.4	1.00
10mm/min	7	0.1407	0.76	0.18	185.13	5.37	10.74	1.72
10mm/min	8	0.1781	0.76	0.23	234.34	6.44	12.88	1.82
10mm/min	9	0.1494	0.76	0.19	196.58	5.45	10.9	1.80
10mm/min	10	0.1721	0.76	0.23	226.45	13.97	27.94	0.81
10mm/min	11	0.1328	0.76	0.17	174.74	11.86	23.72	0.73
10mm/min	12	0.1667	0.76	0.22	219.34	6.07	12.14	1.81
10mm/min	13	0.1307	0.76	0.17	171.97	10.88	21.76	0.79
10mm/min	14	0.1513	0.76	0.19	199.08	5.97	11.94	1.67
10mm/min	15	0.1478	0.76	0.19	194.47	8.51	17.02	1.14
10mm/min	16	0.1598	0.76	0.21	210.26	5.92	11.84	1.77
10mm/min	17	0.1608	0.76	0.21	211.58	7.34	14.68	1.44
10mm/min	18	0.1086	0.76	0.14	142.89	8.14	16.28	0.87
10mm/min	19	0.1504	0.76	0.19	197.89	9.64	19.28	1.02
10mm/min	20	0.1604	0.76	0.21	211.05	7.74	15.48	1.36
10mm/min	21	0.1817	0.76	0.24	239.08	9.04	18.08	1.32
10mm/min	22	0.1849	0.76	0.24	243.29	8.95	17.9	1.36
10mm/min	23	0.1244	0.76	0.16	163.68	6.32	12.64	1.29
10mm/min	24	0.1654	0.76	0.22	217.63	7.4	14.8	1.47
10mm/min	25	0.1188	0.76	0.17	156.31	6.97	13.94	1.12
10mm/min	26	0.1633	0.76	0.21	214.87	7.97	15.94	1.35
10mm/min	27	0.1671	0.76	0.22	219.87	9.36	18.72	1.17
10mm/min	28	0.1532	0.76	0.20	201.58	6.63	13.26	1.52
10mm/min	29	0.1783	0.76	0.23	234.60	7.43	14.86	1.58
10mm/min	30	0.1537	0.76	0.20	202.24	7.44	14.88	1.36
Average Strength and Strain					**201 MPa**		**16.50%**	**1.29**

Appendix D

Distribution of the maximum load at break of LDTF and SGF

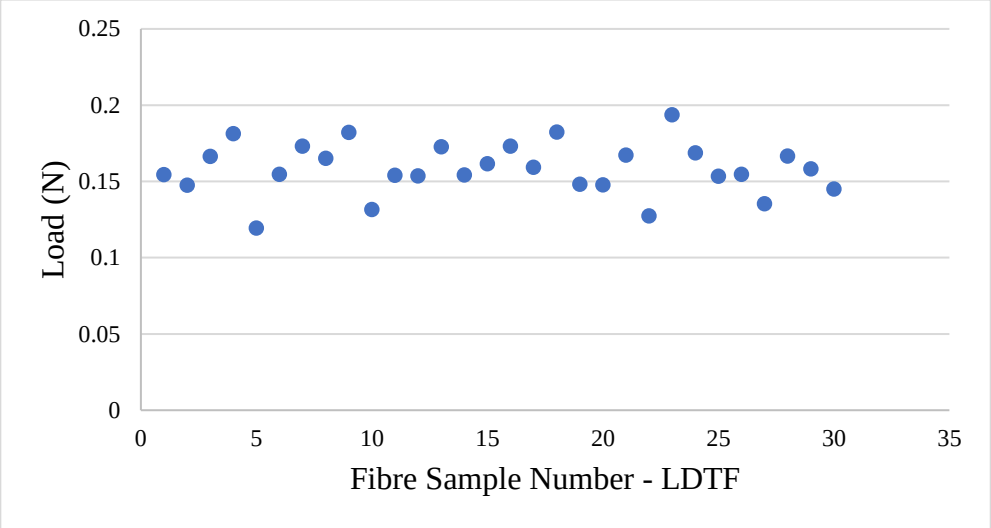

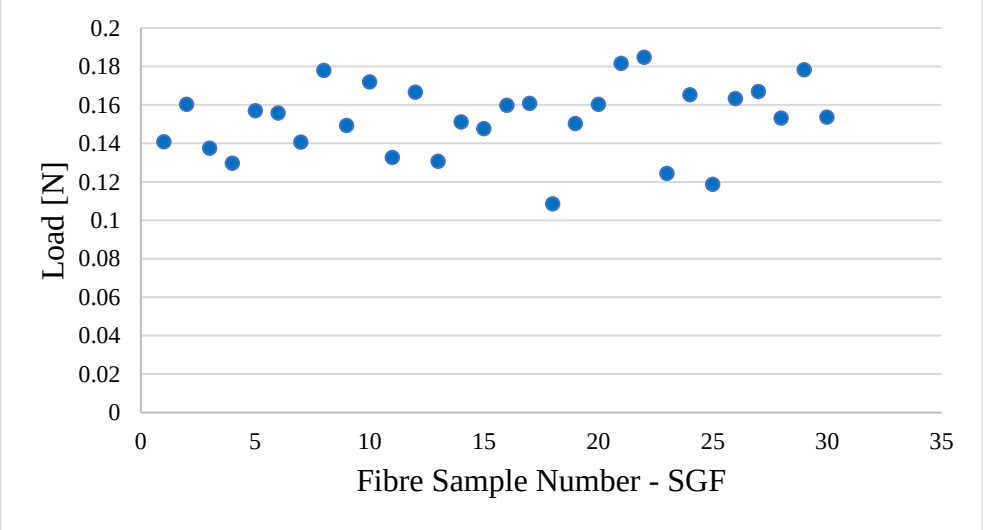

Appendix E

Distribution of the elongation of LDTF and SGF